Plant growth, development and lignification affected by the cationic cell-wall-bound peroxidase (CWPO-C) via auxin catabolism in transgenic Arabidopsis thaliana and Populus alba

ヨシカイ ベニテス ディエゴ アロンソ

Plant growth, development and lignification affected by the cationic cell-wall-bound peroxidase (CWPO-C) *via* auxin catabolism in transgenic *Arabidopsis thaliana* and *Populus alba*

Diego Alonso Yoshikay Benitez

2023

Kyushu University

ACKNOWLEDGEMENT

I would like to extend my gratitude to our Almighty God who made this study successful and gave me strength at all times.

I am extremely grateful to my supervisor, Prof. Yuji Tsutsumi for his invaluable advice, continuous support, and patience during my PhD study. His immense knowledge and plentiful experience have encouraged me all the time of my academic research and daily life. I would also like to thank Prof. Koki Fujita, Prof. Yoshio Kijidani and Dr. Jun Shigeto for their knowledge and research support on my study.

Additionally, I want to express my deepest and immense gratitude to The Ministry of Education, Culture, Sports, Science and Technology (MEXT) for the scholarship and financial support during my Ph.D. study.

I would like to thank all the members in the Laboratory of Forest Chemistry and Biochemistry, since the completion of this work could not have been possible without the help and support that I got from them during my study period in Japan. Also, it is their kind help and support that have made my study and life in the Japan a great time.

Finally, I would like to express my gratitude to my family and my friends. My sincere admiration, appreciation and gratitude to my sister, who fights a terrible illness, for her unconditional support and her sacrifice during the completion of my Ph.D. Without my family and friends tremendous understanding and encouragement in the past few years, it would be impossible for me to complete my study.

Table of Contents

Abbreviations

CWPO-C	cationic cell-wall-bound peroxidase;
IAA	indole-3-acetic acid
GUS	β-glucuronidase
RNAi	RNA interference
OE	overexpression
LC-MS/MS	liquid chromatography–tandem mass spectrometry
LMD	laser micro-dissection
RT-qPCR	real-time quantitative
PCR	polymerase chain reaction
ABSL	acetyl bromide-soluble lignin
DFRC	derivatization followed by reductive cleavage
GC-FID	gas chromatography flame ionization detector
S/G ratio	syringyl/guaiacyl ratio

Chapter 1: Introduction

1-1. Lignin

1-1-1. Composition, bonds and function of lignin

The structure of lignin is complex, forming clusters with aromatic heteropolymers, and it is composed of phenylpropanoic units derived from three cinnamyl alcohols: *p*-coumaryl (H), coniferyl (G) and sinapyl (S) alcohol (Freudenberg and Neish, 1968). Environmental and growth conditions influence the amount and composition of lignin, as well as the plant species, cell type and tissue (Campbell et al., 1996). Dicotyledonous plants divided into angiospermics (hardwood) and gymnospermics (softwood) have different levels of G, S and H units, hardwood contains mainly G, S and traces of H units, while softwood is composed of G units with low levels of H units. In the case of monocotyledonous plants (grasses), the opposite composition occurs; there are more H units than G and S units.

These phenylpropanoid alcohols are interconnected by bonds such β-5, β-β, 5-5, 5-*O*-4 and β-1, which are more resistant to chemical attack, or β-*O*-aryl ether bonds (β-*O*-4). The abundance of each bond type is directly proportional to the amount of monomers in the polymer. If a lignin sample is composed mainly of G units, it will have a higher number of β-5, 5-5, and 5-*O*-4 bonds due to the availability of monolignols for coupling, which makes softwoods lignin more resistant to degradation.

The main functions of lignin is to stiffen the secondary cell wall, make the cell wall hydrophobic and protect the plant from stress. First, the secondary cell wall structure is composed of cellulose and hemicellulose that form reinforced fibers when interlaced with lignin. This matrix confers rigidity and support to vascular plants allowing plants to develop

(Sarkanen and Ludwig, 1971). Second, the characteristic hydrophobicity of the lignin polymer confers properties and conditions suitable to the cell wall for the transport of water and nutrients. Third, it was shown that lignin is synthesized in greater quantities in plants attacked by pests and diseases, by accumulation of H units, the cell wall thickens and prevents the infiltration of fungi and toxins (Zhang et al., 2007; Santiago et al., 2013). Likewise, lignin confers tolerance to droughts, saline stress and climatological stress, in the previous cases, cells synthesize and deposit a greater amount of monolignols in the cell wall, this thickening of the wall avoids water losses due to perspiration and breaking of the cell membrane by cavitation.

1-1-2. Lignin deposition in the cell wall

The way in which the lignin is deposited in the cell wall is given in a gradually manner, as the formation of each layer of cell wall is completed. Once the formation of S2 is completed with cellulose deposits, the deposition of lignin begins in S1. The cell wall is composed of primary cell wall (little lignified), the three layers of secondary cell wall (S1, S2 and S3) named them from the outermost to the innermost of the lumen.

Although the middle lamella contains the highest concentration of lignin deposited especially in the cell corners, the S2 cell wall contains the highest abundance of the hydrophobic polymer. In the case of the deposited order, in angiosperms H units are deposited first, followed by G units, and finally S units. Likewise, the type of cells have different ratios of monomers, for example in angiosperms the case of vessels, they have more G units and in the case of fibers and parenchymal rays the opposite, a greater number of S units.

1-1-3. Monolignol biosynthesis pathway

For the synthesis of monolignols it is needed the participation of 14 enzymes. monolignols synthesis occurs in two pathways, the shikimate pathway carried out in the plastid and the phenylpropanoid pathway undertaken in the cytoplasm (Weinstein et al. 1962, Schmid and Amrhein 1995).

The monolignols biosynthesis process starts from the phenylalanine molecule. Phenylalanine is subjected to deamination, hydroxylation of the aromatic rings, formation of methoxy groups and reduced alcohol group of the carboxilic group. Such is the case of the ferulate-5-hydroxylase (F5H) enzyme, which initially it was estimated that its hydroxylative function acted on ferulic acid, coniferyl aldehyde and coniferyl alcohol, but it was confirmed that the preferential substrate of F5H is coniferyl aldehyde and alcohol (Osakabe et al. 1999). Likewise, the COMT enzyme is capable of methoxylation of caffeic acid, caffeyl aldehyde, caffeoyl alcohol, but shows greater affinity for the substrates 5-hydroxyferulic acid, 5-hydroxyconiferyl aldehyde and 5-hydroxyconiferyl alcohol (Osakabe et al. 1999, Li et al. 2000, Parvathi et al. 2001).

The last step to obtain coniferyl alcohol is taken by reduction of coniferyl aldehyde by means of the CAD enzyme. Obtaining sinapyl alcohol is carried out by a CAD homolog, SAD, which in plants like Poplar is common to observe increases in sinapyl alcohol due to its reducing activity (Li et al. 2001). CAD and SAD have different degrees of activity depending on the plant species. It was also discovered that in the case of *Robinia*, molecules of sinapic acid were found in its lignin, while in the case of Arabidopsis no signal of sinapic acid could

be found in its lignin (Yamauchi et al. 2003). Homologs of the S-CoA ligase enzyme 4CL in *Robinia* have the particularity of preferring sinapic acid as substrate, instead of ferulic acid, caffeic acid or *p*-coumaric acid.

Finally, after the monolignols are synthesized, they are transported to the cell wall to be polymerized and become part of the lignin. Xylem cells are highly lignified, and their cell walls have the highest lignin density in the plant. First, monolignols accumulate in the cytoplasm as in glycosylated form (Steeves et al. 2001) to later be transported passively by Golgi vesicles or actively using ABC transporters (Samuels et al. 2002).

1-1-4. Dehydrogenative polymerization of lignin

After monolignols are delivered to the cell wall, monolignols are incorporated into the lignin polymer through dehydrogenative polymerization (Sarkanen and Ludwig, 1971). The dehydrogenation of monolignols occurs in the presence of enzymes, such as peroxidases, laccases and polyphenol oxidases. It was observed that lignin formation increased in the presence of H_2O_2 (Olson and Varner, 1993), which let suppose that peroxidases are the main enzymes during the formation of dehydropolymerizates monolignols.

1-2. Plant growth

1-2-1. Plant growth regulators

In nature, there are external and internal factors that regulate the growth of the plant. Among the external factors there are temperature, water availability, saline stress, etc., and within the

internal factors is the balance of nutrients and one of the most important: hormones. There are hormones that enhance growth, seed germination, axillary bud dormancy outgrowth, etc., among them it is worth highlighting auxins, gibberellins, brassinosteroids, strigolactones, cytokinins, ethylene, jasmonates and salicylic acid. Also, there are hormones that negatively regulate growth such as abscisic acid, which induces leaf senescence, etc. Likewise, it is possible to understand the interactions that occur between the hormones themselves, regulating each other (Davies 2010). It is known that axillary buds are activated by a decrease in basipetally transported auxins in the stem, which induces sporadic cell division in axillary buds, this division occurs after the increase of cytokinins in the mentioned organs (Bredmose and Costes, 2003). Thus, in modern agriculture, these hormones are used to increase the growth of crop plants or to break the dormancy of seeds.

Phytohormones have action over cells usually on specific growth stages, their effect are greater in these stages compared to previous or later stages. Some hormones are produced *in situ*, that is to say within the same organ in which the hormone will act and be active; another hormones move to another organ following a concentration gradient or active transport.

1-2-2. Auxin

Within plant growth regulators, auxins is one major plant hormones and the first to be discovered. Auxin has different concentrations between organs. The concentration of auxins in each organ determines the development of the plant, moreover the concentration is regulated by it metabolism and transport. Therefore, an auxin maxima and minima

concentration in the whole plant is generated naturally. The difference of concentration between the auxin maxima and minima shapes and determines the plant morphology.

The synthesis of free auxins can occur in two ways, *de novo*, it refers when the hormone is synthesized from its precursor tryptophan (trp), or the hydrolitic way of auxin-conjugated forms, when by a hydrolitic reaction auxin is deconjugated of amino acids, sugars or methyl esters. There are several types of auxins in nature, indole-3-acetic acid (IAA), 4-chloiroindole-3-acetic acid (4-Cl-IAA), phenylacetic acid (PAA), etc., among them, the first to be discovered and most abundant is the IAA (Ludwig-Müller J, 2011).

1-2-3. Auxin phenotype: leaf hydathodes and gravitropism

We know that auxins are synthesized in greater quantity in the shoot apex. This determines the aerial growth of the plant, the apical dominance and the tropisms to which the plant can be affected. Also, it should be announced that *in planta* there are organs that synthesize free-auxin (axillary meristems outgrowth and leaf hydathodes), which can determine the morphology of the plant (Bredmose and Costes, 2003; Aloni et al. 2003).

IAA is a limiting factor in the formation of xylem in leaves, as demonstrated by Sieburth (1999) when applying auxin transport inhibitors to leaves. The inhibitors resulted that the venation of the leaves were formed irregularly, having a greater effect on the young leaves. At the time, venation patterns were poorly understood, Aloni (2001) hypothesized the leaf-venation mechanism where auxin regulates morphology of dicotyledonous leaves. Furthermore, it was shown that hydathodes produce free-auxin during leaf formation, independently of the shoot apex (Aloni et al. 2003).

The process of gravitropism is a complex mechanism that redirects the organs of the plant in order to continue its vertical growth. By subjecting a plant to a gravitational angle that does not correspond to the gravitational vertical vector of the stem or roots, the sensory organ (stem apex) sends a signal to the response organ (stem), thus modifying the anatomy and morphology of the stem. These signals are based on auxins, according to the Cholodny-Went hypothesis (Went and Thimann, 1937), which suggests that auxin accumulates differentially in the stem, thus causing cell division which evoking curvature in the appropriate gravity vector. Similar to what happens with phototropism and apical hook formation (Schwark and Schierle, 1992). Although it is difficult to determine the differential accumulation of auxins in certain cases, through various studies using Arabidopsis mutants it has been possible to clarify that auxin is an essential hormone in the tropism process (Blancaflor and Masson, 2003; Muday and Murphy, 2002).

Analytical techniques or bioassays helped to quantify or locate IAA. It is necessary to quantify IAA *in situ* of action during gravistimulation. One of the first techniques, to determine the transportation of auxins was to apply in the excised plant stems IAA embedded in agar, in order to diffuse the hormone through the stem. Then, with the advancement of radiolabeled techniques, trials with radiolabeled IAA were performed, showing consistent evidence about the distribution of auxin in the organ with bend curvature (Pickard, 1985). Even so, this accumulation did not determine whether the accumulation of auxin was the product of curvature or whether auxin was responsible for such asymmetry (Muday, 2001).

It was not until the last few years that a better insight was obtained, in regards of the effect that auxin had over the bend stem during gravitropism. By means of *in situ* techniques, GC-MS or LC-MS-MS were used to quantify auxin levels precisely (Bandurski et al. 1984, Kowalczyk and Sandberg 2001); and gene reporter system such as *DR5*::*GUS* (Ulmasov et al. 1997) detected as a reporter gene the accumulations of auxin. By both mentioned techniques, it was possible to determine the spatio-temporal relationship between auxin and the bent stem. Although the accumulated auxin gradients in the bend curvature zone are transient, it seems to be sufficient to activate the downstream mechanism leading to the bending response.

1-2-4. IAA and Class III peroxidase

The most known catabolite of IAA is 2-oxoindole-3-acetic acid (oxIAA), the oxidized form of IAA. This catabolization process is considered irreversible, and is not transported by gradient through the plant. The old-known enzyme responsible for the oxidation of IAA are two dioxygenases (DAO1 and DAO2), which act on auxin homeostasis, interacting with GH3 genes to maintain optimal auxin levels for plant growth and development (Zhang et al. 2016). However, in the absence of DAO, IAA does not accumulate in excess as expected; homeostatic mechanisms maintained regulated IAA by conjugation, generating large amounts of IAA-conjugated.

Another disfunctioning way of IAA is the oxidative decarboxylation of IAA by plant peroxidases was reported decades ago. As stated by Gaspar et al. (1994), the cationic peroxidases could be the main responsible for IAA oxidation. IAA incubated with HRP

peroxidase showed different oxidation products as oxIAA (Hinman and Lang, 1965). Two oxidating mechanisms pathway for *in vitro* IAA oxidation by HRP-C were proposed: (a) peroxidative cycle (native enzyme → compound I → compound II → native enzyme) and (b) ferrous enzyme / compound III shuttle (native enzyme → ferrous enzyme → compound III → ferrous enzyme). Ferrous enzyme / compound III shuttle is the most accepted scheme because oxidation is carried at low ratios of peroxidase (Gazaryan et al. 1996). Plant peroxidases towards IAA behave "alike" oxygenases with high substrate specificity. Peroxidase common products are 3-alkylideneoxindoles which derived from oxidation of 3-alkylindoles (Hinman and Lang, 1965).

1-3. Plant peroxidase

1-3-1. Peroxidase definition and classification

Classification of peroxidase superfamily was proposed by Welinder (1992), who state that peroxidases belong into three families (class I, II, and III) by sequence homology. Class I, represents the intracellular peroxidases, includes yeast cytochrome c peroxidase (CCP), ascorbate peroxidase (AP) and bacterial catalase-peroxidases. Class II is represented by the secretory fungal peroxidases such as lignin peroxidase (LiP) and manganese peroxidase from *Phanerochaete chrysosporium*, and *Coprinus cinereus* peroxidase or *Arthromyces ramosus* peroxidase (ARP). The main role of class II peroxidases is the degradation of lignin in wood. Class III, catalize classical secretory plant peroxidases, encode large number of genes per plant species, e.g., 73 genes in *Arabidopsis thaliana* and 93 genes *Populus trichocarpa*.

Implying that Class III peroxidases have a diverse range of functions. Class III plant peroxidases (EC 1.11.1.7) are heme-containing oxidative plant enzymes encoded by multigene families (Welinder, 1992). The majority are localized in the cell wall or the vacuole. Peroxidases can oxidize a wide range of substrates at the expense of H_2O_2.

1-3-2. Peroxidative catalytic cycles

Compound I derived from plant or fungal peroxidase is defined to have oxo-ferryl porphyrin π-cation radical structure of heme (Dolphin et al. 1971). Compound II, formed by one electron reduction of compound I by RH reducing substrate, has oxo-ferryl structure of the heme (Theorell and Ehenberg, 1952; Moss et al. 1969; Sitter et al. 1985). Normally, the reduction of compound I to resting state occurs via intermediate formation of compound II through the oxidation of two substrates. But under particular condition, Class III peroxidase is known to cause the other type of reaction in which peroxidase compound I is reduced directly back to resting enzyme. These reactions were observed in the oxidation of iodide and sulfite (Araiso et al. 1976, Kobayashi et al. 1987), and the sulfoxidation of thioether (Harris et al. 1990). In case of ROS accumulation stress conditions, Compound III is formed, by reduction of hydrogen peroxide to water, next compound III is reduced to the resting state by the action of another hydrogen peroxide molecule. In some cases superoxide anion formed by the oxidation of R• could lead to the formation of Compound III from the enzyme resting state directly, in order to reduce hydrogen peroxide (Figure 1-1.).

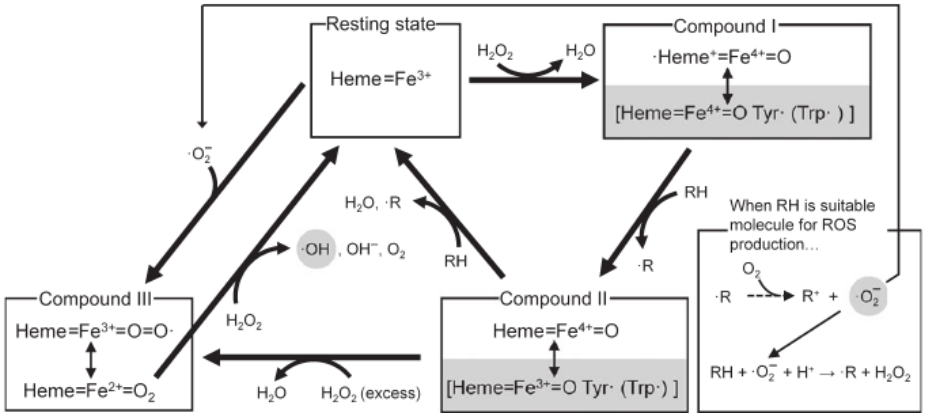

Figure 1-1. Class III peroxidase cycle. Shigeto and Tsutsumi 2016.

1-3-3. Peroxidases and lignification

Substrates are broad for the peroxidases that participate in the lignification process, but one of the monomers that make up the lignin polymer, sinapyl alcohol, does not have a wide spectrum of peroxidases that can oxidize it. Monolignols such as *p*-coumaryl alcohol, coniferyl alcohol show well bind to the substrate-binding residues of most peroxidases such as ATP A2 (Østergaard et al. 2000). This is because the Pro-139 residue of most peroxidases overlaps with the 5-methoxy group of sinapyl alcohol, thus not allowing radicalization of sinapyl alcohol (Østergaard et al. 2000). However, peroxidases that have a preference towards sinapyl alcohol have been reported (Tsutsumi et al. 1994, Aoyama et al. 2002, Barceló et al. 2001, Gabaldón et al. 2005, Marjamaa et al. 2006). The first peroxidase to be reported to efficiently oxidize sinapyl alcohol compared to coniferyl alcohol was Poplar cationic cell-wall-bound peroxidase (CWPO-C) (Tsutsumi et al. 1994, Aoyama et al. 2002). CWPO-C has Tyr74 and Tyr177 residues that act as catalytic sites for sinapyl alcohol and lignin polymer (Sasaki et al. 2008, Shigeto et al. 2012). These tyrosine and tryptophane residues, similarly found in Class II peroxidases, are considered long-range electron transfer (LRET) that act as alternative oxidation sites, which confers to CWPO-C peroxidase a very particular evolutionary characteristic. Then, ZePrx34.70 and ZePrx33.44 from *Zinnia elegans* showed to oxidize sinapyl alcohol between the monolignoles *p*-coumaryl alcohol, coniferyl alcohol and sinapyl alcohol (Gabaldón et al. 2005). Lastly, BPX1 from *Betula pendula* was found to prefer sinapyl alcohol over coniferyl alcohol (Marjamaa et al. 2006).

The peroxidases that participate in the lignification process are divided by their isoelectrophoretic nature into anionic, neutral and cationic. In the beginning it was found that

anionic peroxidases in tobacco were quite active in the polymerization of coniferyl alcohol (Mäder et al. 1977). Followed, studies by Osakabe et al. (1995) showed that the anionic peroxidase of *Populus kitakamiensis* PrxA3a transcribed in high amounts when xylem formation occurred. Antisense PrxA3a of Poplar hybrid (*P. sieboldii* x *P. gradidentata*) showed decreased amounts of lignin compared to wild type (Li et al. 2003). These results demonstrated that anionic peroxidases were important in the lignification process. Until Blee et al. (2003) demonstrated with an antisense approach that the cationic TP-60 peroxidase reduced the lignin content by 40-50% compared to the control. It is clear that both anionic and cationic peroxidases participate in the polymerization of lignin.

The lignin in the secondary cell walls of fiber cells is mostly formed of syringyl lignin, and the middle lamella and the vessel walls is mostly formed of guaiacyl lignin in angiosperm walls (Goring et al. 1988; Donaldson, 1991). Therefore, the formation of fiber vessels cell walls conformed of sinapyl alcohol depends entirely on a peroxidase that can efficiently radicalize S monomer. Hence, it is proposed that the discovery of CWPO-C, which can efficiently oxidize sinapyl alcohol, allows woody angiosperm to grow in nature (Tsutsumi et al. 1994).

1-3-4. Peroxidases and plant growth

Some Class III peroxidases are know to participate in plant growth and developmental processes. The AtPrx33 and AtPrx34 promote root elongation. In absence of AtPrx53 the hypocotyl elongates (Jin et al. 2011). The CpPrx01 from *Cucurbita pepo* resulted to be involved in roots and hypocotyls elongation, with alteration of the IAA (Cosio et al. 2009).

As previously mentioned, IAA was demonstrated to be catabolized by HRP-C. Yet, an *in vitro* approach assay showed that oxidative scission of cell wall could be induced in the presence of ROS, specially the hydroxyl radicals (•OH) (Lizkay et al. 2004). Then, Müller et al. (2009) *in vivo* assay demonstrated that cell wall scission by •OH occurred in maize coleoptiles. It is known that •OH are generated during the peroxidase reaction. Therefore, in case of roots, class III peroxidases appears to participate by two ways: oxidation of IAA and/or •OH generation.

1-4. The aim of this study

Plant peroxidases are able to dehydrogenative polymerize lignin and monomers. Before Tsutsumi et al. (1994), it was not discovered a peroxidase which could dehydrogenative polymerize syringyl lignin. Later, it was determined *in vitro* that unique Class III peroxidase, CWPO-C, was able to efficiently oxidize sinapyl alcohol and lignin polymer for lignification (Aoyama et al. 2002, Sasaki et al. 2004). According to the "End-wise polymerization" process, monolignols couple with the pre-polymers to produce lignin (Sarkanen and Ludwig, 1971). Still, it was not proved whether CWPO-C oxidize the syringyl and pre-polymers *in vivo*. Therefore, by the use of *CWPO-C* transgenics, the effect of CWPO-C in lignification was studied in this work.

In Chapter 2, it was presented that *CWPO-C* promoter was expressed in xylematic and meristematic tissues. By the use of GUS reporter gene inserted in Arabidopsis plant, it was revealed that CWPO-C was located in young xylem tissues, and unexpected meristematic

tissues such apical meristem and root tips. The aim of this *in vivo* study was to characterize the tissues and plant age where *CWPO-C* promoter expressed. Moreover, it was observed the *CWPO-C* overexpression affected the plant height. These findings lead to postulate that *CWPO-C* was expressing in not-aim to lignification tissues. Thus, it seemed to be involved in growth hormone catabolization.

In Chapter 3, it was clarified that CWPO-C can catabolize the IAA *in vitro* and *in vivo* conditions. For that reason, it was quantified by LC-MS/MS the amounts of IAA in the *CWPO-C* overexpression Arabidopsis. It was revealed that the amounts of IAA severely decreased by the effects of high *CWPO-C* expression. Also, an *in vitro* reaction between IAA and rCWPO-C complemented *in vivo* results. Therefore, it was of interest to investigate the phenotype of *CWPO-C* overexpression in poplar. Since poplar is the plant where CWPO-C was first isolated.

In Chapter 4, it was presented that *CWPO-C* promoter was expressed in xylematic and meristematic tissues in Poplar, similar to *CWPO-C* promoter expression results as Arabidopsis. By the use of GUS reporter gene inserted in poplar plant, it was revealed that CWPO-C was located in xylem tissues, and meristematic tissues such apical and axillary meristems. The *in vivo* study showed the CWPO-C peroxidase expression patterns. Moreover, it was observed the *CWPO-C* overexpression in Poplar enhanced plant height, differently than in *CWPO-C* overexpression Arabidopsis, where dwarf were generated. These findings lead to postulate that CWPO-C was expressing in xylem and not-aim to lignification tissues. The similar expression patterns of *CWPO-C*, compared in two different plant species let

hypothesize that CWPO-C is to be involved in lignification and growth hormone catabolization.

In Chapter 5, Poplar suppressing *CWPO-C* decreased lignin content strongly. Moreover, S/G ratio was also decreased in the absence of CWPO-C. This *in vivo* results confirmed and are in accordance to the *in vitro* results (Aoyama et al. 2022, Sasaki et al. 2004). Thus, it is confirmed that in nature CWPO-C is responsible for oxidize monolignols and lignin pre-polymers.

Chapter 2: *CWPO-C* expression through plant growth and aim to lignification tissues in Arabidopsis

2-1. Introduction

Plant peroxidases (EC 1.11.17, Class III peroxidases; Prxs) are plant-specific heme oxidoreductases comprising approximately 300 amino acid residues. Land plants contain many genes encoding Prxs localized in the apoplast or vacuole (Zipor et al. 2013). Peroxidases catalyze reactions affecting several important physiological and developmental processes (e.g., lignification, stress responses, development, and germination), with diverse substrate specificities and reactivities. However, the function and the substrate of most Prxs remain unidentified. Thus, the available information regarding the mechanism underlying the *in vivo* activity and role of Prxs is limited. Regarding lignin polymerization (i.e., lignification), a repeating radical coupling of a new monomer to the growing polymer (or oligomer) in the cell wall occurs via oxidative coupling. Lignin is composed of three major monolignols, namely *p*-coumaryl alcohol, coniferyl alcohol, and sinapyl alcohol. This oxidative coupling mechanism is catalyzed by Prxs and/or laccase.

Peroxidases can catalyze the oxidation of a broad range of substrates. The well-studied Prxs Horseradish peroxidase isoenzyme C (HRP-C) and AtPrx53 minimally oxidize sinapyl alcohol and the lignin oligomer because these potential substrates are larger than the heme pocket of these two enzymes. However, we previously reported that the cationic cell-wall-bound Prx (CWPO-C) from *Populus alba* can efficiently oxidize lignin monomers, including sinapyl alcohol, and high molecular weight lignin polymers (Aoyama et al. 2002, Sasaki et al. 2004). This unique oxidation is facilitated by the fact that the oxidation sites (Tyr74 and Tyr177) of CWPO-C are located on the protein surface, enabling the enzyme to avoid steric hindrance during enzyme–substrate interactions (Shigeto et al. 2012). This finding suggests

that the formation of lignin containing sinapyl alcohol in the cell wall can be catalyzed by a certain type of Prx, including CWPO-C. Furthermore, we reported that the putative *Arabidopsis thaliana* (Arabidopsis) homologs of CWPO-C, AtPrx2, AtPrx25, and AtPrx71 (48%, 66%, and 68% amino acid identity with CWPO-C, respectively), can also oxidize sinapyl alcohol and lignin polymers (Shigeto et al. 2014). Silencing *AtPrx2*, *AtPrx25*, and *AtPrx71* affects lignin-related phenotypes by decreasing the lignin content and/or changing the lignin structure (Shigeto et al. 2013, 2015).

The results of earlier studies suggested that CWPO-C is responsible for the lignification process in stem. In this study, we further characterized the possible *in vivo* function of CWPO-C on the basis of a spatiotemporal analysis of gene expression using transgenic plants expressing *β*-glucuronidase (GUS) under the control of the *CWPO-C* promoter as well as a phenotypic analysis of *CWPO-C*-overexpressing (OE) Arabidopsis lines. Unexpectedly, our findings revealed that CWPO-C has functions associated with plant growth.

2-2. Materials and methods

2-2-1. Plant materials and growth conditions

Wild-type (WT) and transgenic *Arabidopsis thaliana* (ecotype Columbia) plants were used in this study. Seeds were immersed in 0.5% (v/v) sodium hypochlorite for 5 min and then rinsed three times with sterile water. After imbibition at 4°C for 1 day, the seeds were sown in plastic Petri dishes containing Murashige and Skoog (MS) medium supplemented with 3% (w/v) sucrose, pH 5.6, and 0.3% (w/v) gellan gum. The plates were incubated in CLE-303

cultivation chambers (TOMY SEIKO Co., Ltd., Tokyo, Japan) set at 22 ± 1°C with a 16-h light (100 μmol photons m^{-2} s^{-1}):8-h dark cycle. Three-week-old seedlings were transferred to pots containing vermiculite and perlite (1:1, v/v) and were subsequently irrigated with 0.1% Hyponex (Hyponex Japan, Osaka, Japan) every 4 days.

2-2-2. Generation of transgenic plants

The transgenic plants used in this study were Arabidopsis ecotype Columbia background. Complete *CWPO-C* sequence and *CWPO-C* promoter sequence were previously prepared from *Populus alba* (Sasaki et al. 2006). To generate a fusion construct comprising the *CWPO-C* promoter and the *GUS* marker gene (*Pcwpo-c*::*GUS*) (Fig. 2-4a) and a *CWPO-C* overexpression construct consisting of the CaMV 35S promoter (*P35S*::*CWPO-C*) (Fig. 2-4b), the 1,855-bp 5′ upstream region of *CWPO-C* and the complete *CWPO-C* open reading frame were amplified by PCR and then subcloned into the pBluescriptII vector (Qiagen). The PCR primer sequences were as follows:

P_{CWPO-C}-left (5′-gcgcaagcttagggaaacaactaaaataccattaataac-3′) and

P_{CWPO-C}-right (5′-gttggatcctgtatatgctagctaagagactg-3′);

CWPO-C-left (5′-cgggatccatgagccaaaaagtagttttaatgtttc-3′) and

CWPO-C-right (5′-ccgagctcatttatagcagaacacactcttcgaatttcac-3′).

For the *Pcwpo-c*::*GUS* fusion construct, the 1,855-bp 5′ upstream region of *CWPO-C* and the *GUS* gene were introduced between *Hind*III and *Bam*HI and between *Bam*HI and *Sac*I, respectively, in the binary vector PBF2 (Nishiguchi et al. 2006). Regarding the *CWPO-C*

overexpression construct, the complete *CWPO-C* open reading frame (Sasaki et al. 2006) was introduced between *Bam*HI and *Sac*I in the PBF2 vector. For each construct, the binary vector was inserted into *Agrobacterium tumefaciens* strain LBA4404 cells, which were then used to transform plants according to the floral dip method (Clough and Bent 1998). The transgenic plants were selected on half-strength MS medium supplemented with 50 mg L^{-1} kanamycin. Seeds were collected from each kanamycin-resistant F_1 plant. Homozygous T_2 plants were identified and selected according to the proportion of kanamycin-resistant plants. Homozygous T_3 and T_4 transgenic plants were used for further analyses.

2-2-3. Western blot analysis

Whole aerial plant parts without roots from 2-week-old WT and transgenic Arabidopsis seedlings, grown in Petri dishes containing MS medium were collected and frozen in liquid nitrogen. Later, the ground powder was mixed with 3 equivalent volumes (w/v; mg μL^{-1}) of sodium dodecyl sulfate (SDS) sample buffer containing 50 mM Tris-HCl (pH 7.4), 2% SDS (w/v), 6% β-mercaptoethanol (v/v), 10% glycerol (v/v), and 0.001% bromophenol blue and then homogenized. The homogenate was centrifuged at 20,000 *g* for 20 min. The protein content in the supernatant was determined using the Pierce 660 nm Protein Assay kit (Thermo Fisher Scientific).

A 10 μg protein sample was separated by 10% (w/v) SDS polyacrylamide gel electrophoresis and then electroblotted onto a PVDF membrane (Thermo Fisher Scientific). To confirm the equal loading of protein, an identical gel was prepared and stained in parallel with Coomassie brilliant blue. The CWPO-C protein was detected using an anti-CWPO-C antibody and the

anti-rabbit IgG secondary antibody conjugated with horseradish Prx (Proteintech Group Inc.) at a dilution of 1:500 (v/v) and 1:2000 (v/v) in phosphate buffer (pH 7.4), respectively. The anti-CWPO-C antibody was purified from the serum of rabbits immunized with purified recombinant CWPO-C that was prepared by GENE NET (Fukuoka, Japan) as described by Shigeto et al. (2012). The antigen–antibody complex was visualized using AE-1490 EzWestBlue (ATTO).

2-2-4. GUS staining

Transgenic plants were analyzed for GUS staining using a modified version of a published procedure (Jefferson et al. 1987). Briefly, seedlings were treated with 90% cold acetone and incubated for 1 h at − 20°C to remove chlorophyll. After washing twice with 100 mM phosphate buffer (pH 7.4), the seedlings were transferred to the GUS staining solution containing 100 mM $NaPO_4$ (pH 7.4), 0.5 mM 5-bromo-4-chloro-3-indolyl-β-D-glucuronide, 2.5 mM $K_3[Fe(CN)_6]$, and 2.5 mM $K_4[Fe(CN)_6]$. After vacuum infiltration at − 0.6 MPa, the seedlings were incubated at 37°C for 14 to 16 h. The seedlings were washed with the following solutions: 70% ethanol for 30 min, an ethanol:acetic acid solution (9:1, v/v) for 2 h, 90% ethanol twice for 30 min each, and a chloral hydrate:water:glycerol solution (25:9:3, w/v/v) for 4 to 12 h. Stem cross-sections of 15 μm thickness were prepared by cryosectioning using the Tissue-Tek® OCT compound (Sakura-Finetek).

2-3. Results

2-3-1. *CWPO-C* is expressed throughout Arabidopsis and is associated with plant development

A previous RT-qPCR analysis (Sasaki et al. 2006) revealed the *P. alba CWPO-C* gene, which encodes a Class III Prx, is expressed in the xylem, shoot, and leaf. To determine more precisely where and when *CWPO-C* is expressed during plant development, a construct harboring the *GUS* gene under the control of the *CWPO-C* promoter was introduced into Arabidopsis. The staining results indicated *GUS* was expressed in growing organs and tissues that will undergo lignification. The GUS activity was detected in several developing tissues (Fig. 2-1a–f). More specifically, it was observed in the apical meristem (Fig. 2-1b) and developing leaves (Fig. 2-1g), suggesting that *CWPO-C* is expressed in actively growing and/or differentiating cells. Interestingly, we also detected *GUS* expression in the trichome basal cells (Fig. 2-1c), in the stomata (mainly guard cells, Fig. 2-1d, e), and in the hydathodes (Fig. 2-1h) of the developing leaves, implying that CWPO-C may be important for the differentiation of specific organs. Additionally, GUS activity was detected in the young roots, but not at the root tip (Fig. 2-1i), in the young vascular bundles in the upper part of the stem (Fig. 2-1j), in developing seeds (Fig. 2-1l), immature flowers (Fig. 2-1k) and in siliques (Fig. 2-1m), all of which are considered to be undergoing lignification. These observations support our hypothesis that CWPO-C is involved in lignification (Sasaki et al. 2006, Shigeto et al. 2013).

2-3-2. *CWPO-C* negatively regulates Arabidopsis growth

To functionally characterize CWPO-C *in vivo*, we generated transgenic Arabidopsis plants expressing *CWPO-C* under the control of the constitutive CaMV 35S promoter. Three of five

independent lines of *P35S*::*CWPO-C* (OE11, OE12, and OE13), which expressed *CWPO-C* at different levels according to a western blot analysis of the CWPO-C protein (Fig. 2-2a, Fig. 2-3), were subjected to further analyses. Since signals of OE1 and OE9 were weak and similar to OE12, OE1 and OE9 were not considered for further experiments in this study. Among the three transgenic lines OE11, OE12 and OE13, the CWPO-C content was highest in OE11 (Fig. 2-2a). Compared with the WT plants, all three transgenic lines had shorter stems (Fig. 2-2b). Line OE11 exhibited particularly poor stem growth (height and dry weight) (Fig. 2-2c).

Because CWPO-C was most abundant in OE11 plants, this line was characterized further. Interestingly, some OE11 plants exhibited a peculiar phenotypic feature (Fig. 2-2d–f) during the early stages of bolting, not observed in OE12 neither OE13 plants. Specifically, the OE11 apical stem was semi-curled and/or curled (Fig. 2-2e, f), with 60% of the plants in successive generations exhibiting this stem trait (Table 2-1). The OE11 plants with curled and/or semi-curled stems did not produce seeds. The OE11 plants with a straight stem (Fig. 2-2d) produced small fruits with relatively few seeds. Thus, OE11 plants were always derived from plants without curled stems. Western blot and the subsequent determination of band intensities using ImageJ revealed that the OE11 plants with curled stems contained more CWPO-C protein than the OE11 plants without curled stems (Table 2-2). Considered together, these findings indicate that high levels of CWPO-C in Arabidopsis negatively affect plant growth, leading to dwarfism and an abnormal curling phenotype. These results imply that CWPO-C influences the Arabidopsis growth mechanism.

Table 2-1. Proportion of OE11 plants with a curled phenotype in successive generations

Generation	Plants with straight stems	Plants with curled stems	Total number of plants	Curled (%)
1st	9	15	24	63
2nd	13	14	27	52
3rd	19	18	37	49
4th	12	20	32	63
5th	7	11	18	61

Note: The 1st generation is the T_6 generation, which was confirmed as homozygous.

Table 2-2. Integrated band intensity of CWPO-C in the stem tip of OE11 and curled OE11 plants and the relative band intensity of CWPO-C normalized against the intensity of RUBISCO

Phenotype	Average integrated band intensity	Relative integrated band intensity
Curled stem	13,595 ± 508	1.31 ± 0.04
Straight stem	9,638 ± 172	0.97 ± 0.04

Note: The band intensities for the extracted proteins were determined for three biological replicates per phenotype. Data are presented as the mean ± standard deviation.

Table 2-3. Development of 6-week-old *CWPO-C*-overexpressing transgenic and wild-type (WT) Arabidopsis plants

Line	Stem length (cm)	Dry weight ($mg \cdot plant^{-1}$)	Root length (cm)	Number of lateral branches per plant	Number of rosette leaves per plant
OE11	12.9 ± 5.6*	21.6 ± 8.2*	8.0 ± 1.0*	3.4 ± 0.5	10.9 ± 1.3
OE12	24.2 ± 1.5*	31.5 ± 5.8	7.6 ± 1.2*	2.5 ± 0.5	11.1 ± 1.8
OE13	21.8 ± 2.0*	35.0 ± 6.1	7.1 ± 1.2*	3.3 ± 1.1	12.3 ± 1.8
WT	26.2 ± 1.4	35.9 ± 3.4	5.8 ± 1.4	3.2 ± 0.6	11.0 ± 1.3

Note: Data are presented as the mean ± standard deviation (n = 10). Asterisks indicate significant differences between the OE lines and the WT control (*, $p < 0.03$, Student's *t* test).

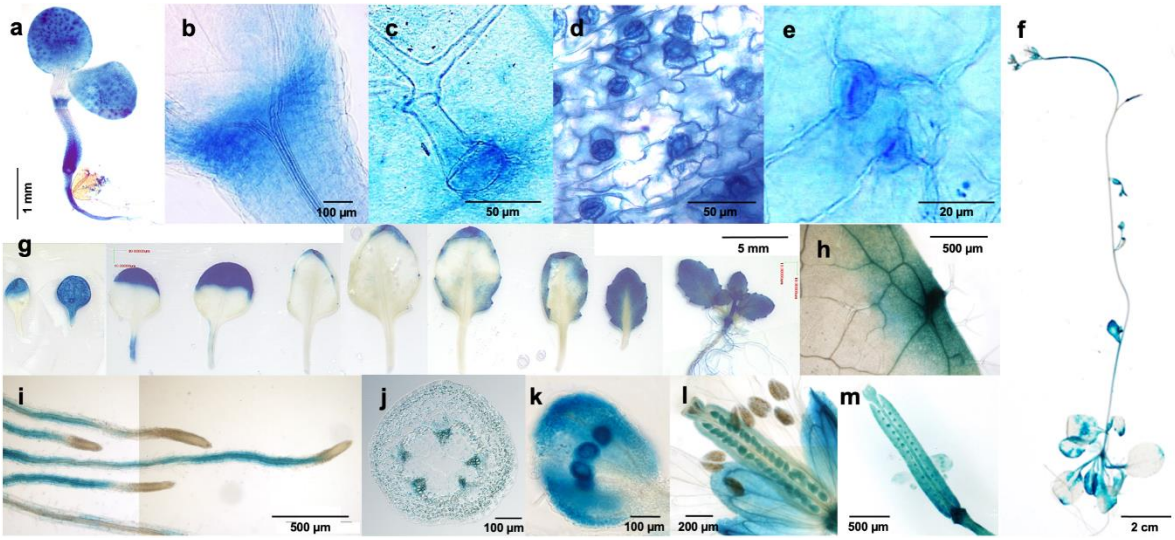

Fig. 2-1. Spatiotemporal expression of *β*-glucuronidase (GUS) driven by the cationic cell-wall-bound peroxidase (*CWPO-C*) promoter in Arabidopsis. **a–e** Analysis of a 2-day-old plantlet. **a** Hypocotyl; **b** Apical meristem; **c** Trichome; **d** and **e** Guard cells. **f** Representative 5-week-old plant. **g** and **h** Leaves from 3-week-old plants. **g** Leaves, left (younger) to right (older); **h** Hydathode. **i** Representative 3-week-old roots. **j** Cross-section of the apical stem of a 6-week-old plant. **k** immature flower. **l** and **m** Representative 6-week-old flower silique. **l** Seed; **m** Silique

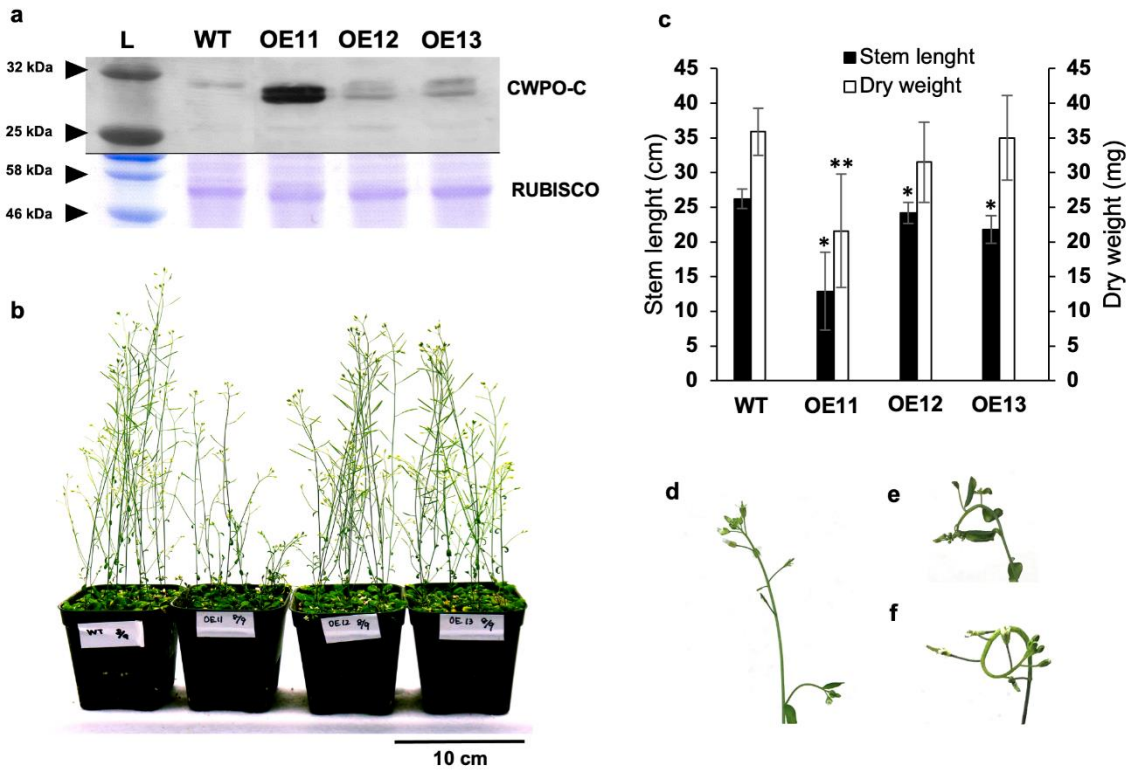

Fig. 2-2. Transgenic *Arabidopsis thaliana* carrying the *P35S*::*CWPO-C* construct. **a** Western blot analysis of CWPO-C-overexpressing transgenic lines 11, 12 and 13 (OE11, OE12, and OE13) and the wild-type (WT) control using an anti-CWPO-C antibody (30 kDa). L: ladder. RUBISCO stained with Coomassie brilliant blue is presented as a reference. **b** Phenotypes of a 6-week-old *P35S*::*CWPO-C* transgenic plant. Dwarfism was characteristic of OE11 plants. **c** Height and dry weight of transgenic lines. Ten biological replicates were analyzed. *: Significant difference ($p < 0.05$) relative to the WT stem length (cm); **: significant difference ($p < 0.05$) relative to the WT dry weight (mg) (Student's *t* test). **d–f** Apical stem phenotypes of OE11 plants. **d** Straight; **e** Semi-curled; **f** Curled

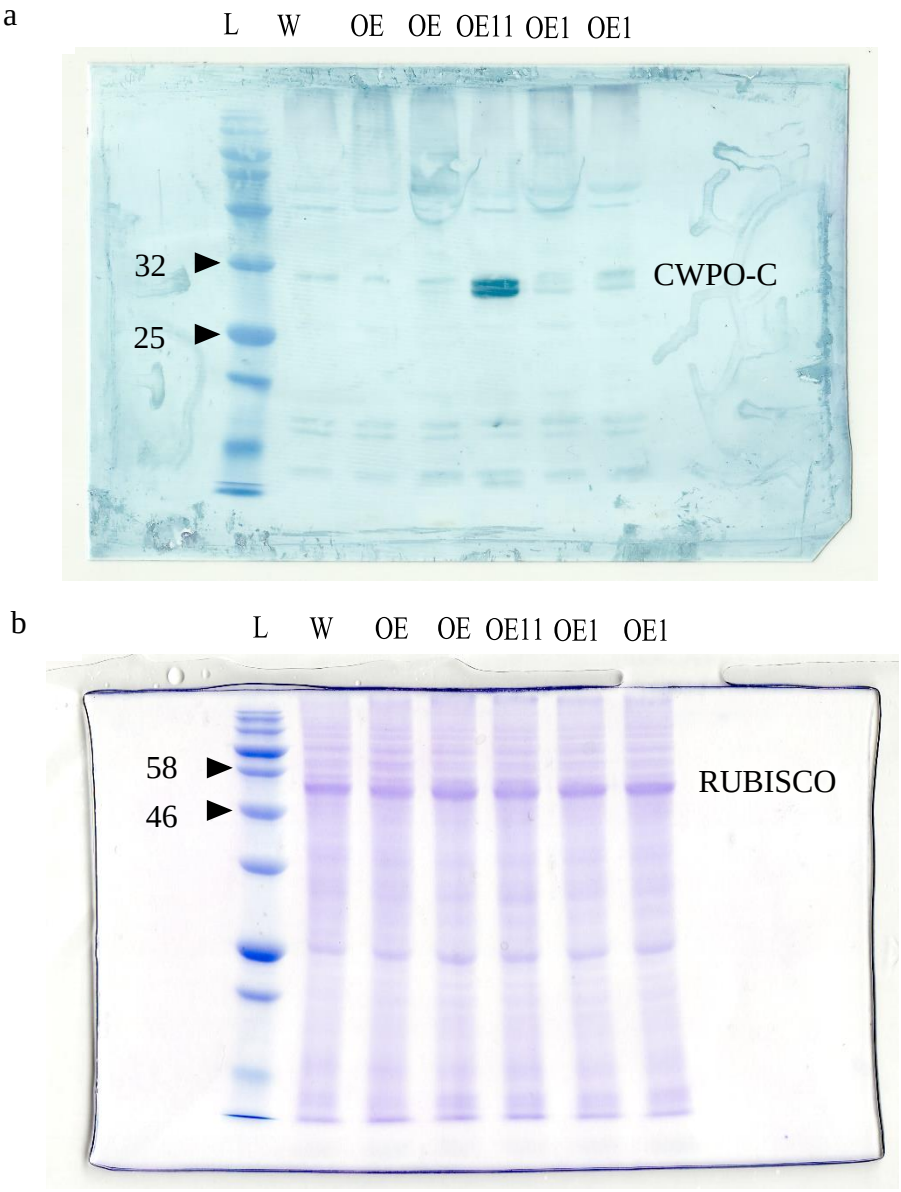

Fig. 2-3 Original gel images of, western blot and CBB analysis (**a** and **b**, respectively), of CWPO-C-overexpressing transgenic lines 1, 9, 11, 12 and 13 (OE1, OE9, OE11, OE12, and OE13) and the wild-type (WT) control using an anti-CWPO-C antibody (30 kDa). L: ladder. RUBISCO stained with Coomassie brilliant blue is presented as a reference

a

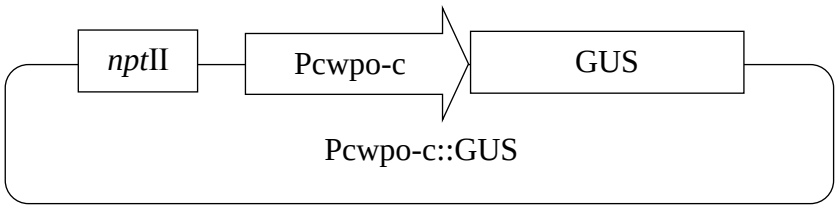

b

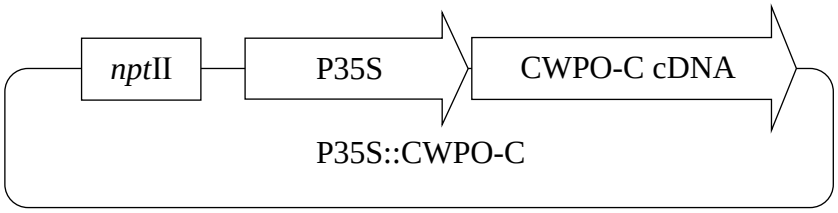

Fig. 2-4 Diagram of construct details for, *Pcwpo-c*::*GUS* and *P35S*::*CWPO-C* (**a** and **b**, respectively)

2-4. Discussion

Earlier research indicated CWPO-C has a versatile oxidizing activity that is unaffected by the substrate size because the oxidation site is exposed on the protein surface (Shigeto et al. 2012), similar to fungal lignin-degrading Prxs (Doyle et al. 1998, Miki et al. 2011, Ruiz-Dueñas et al. 2009, 2009). Additionally, CWPO-C may contribute to lignification because of its unique activity (i.e., ability to oxidize sinapyl alcohol and high molecular weight lignin polymers) (Aoyama et al. 2002, Sasaki et al. 2004). This hypothesis was proposed on the basis of *in vitro* biochemical experiments (Sasaki et al. 2006, 2008); however, there was no direct biological evidence confirming the hypothesis. Lignin provides structural support and is responsible for the hydrophobic properties of water-conducting cells, especially in the xylem. Therefore, the gene encoding a lignification-related Prx is expected to be expressed around tissues in which lignin is being deposited, including xylem and interfascicular fibers. The results of the current study indicated that *CWPO-C* is expressed in the roots, xylem, and silique (Fig. 2-1i, j, m, respectively). This is consistent with the possibility CWPO-C catalyzes lignification. However, *CWPO-C* was also expressed in immature tissues, such as meristems, young upper stems, leaves, flowers, and fruits (Fig. 2-1b, f, g, k and m, respectively). A real time polymerase chain reaction (RT-qPCR) analysis was performed in *Populus alba* L., and the results showed *CWPO-C* expression in shoot, xylem, and leaf (Sasaki et al. 2006), similar to transgenic *Pcwpo-c*::*GUS* Arabidopsis.

Among the transgenic lines overexpressing *CWPO-C*, OE11 had the highest CWPO-C content as well as curled stems, which was an unexpected phenotype. Although the OE11 plants used in this study were homozygous, there were differences in the CWPO-C content

between individual plants. A western blot analysis of the OE11 plants with and without curled stems revealed that the amount of CWPO-C was about 1.3-times greater in the curled stem tip than in the straight stem tip (Table 2-2). Thus, an excessive amount of CWPO-C may cause stem tips to curl and lead to sterility.

2-5. SUMMARY

Investigations were carried out to determine the *in vivo* role of CWPO-C. It was used the Arabidopsis transgenics overexpressing *CWPO-C* and reporter GUS gene with *CWPO-C* promoter. It was found that *CWPO-C* was expressed in the xylem, shoot, young flowers, developing xylem and leaf. The overexpression of *CWPO-C* also affected growth of Arabidopsis, generating dwarf plants with a characteristic auxin deficient phenotype, the curled stem tip. These results suggested that the CWPO-C peroxidase is expressed in not only aim to lignification tissues but also is expressed in meristematic and plant development tissues., which suggests a new role for the peroxidase.

In this Chapter, it was discovered *in vivo*, a new possible role for the CWPO-C peroxidase. Especially, *CWPO-C* expression was located in meristematic tissues, such as stem tip and root tip. This characteristic is quite unique since it shows a double function as the peroxidase. In the next Chapter, the interaction between CWPO-C and growth hormone IAA was investigated.

Chapter 3: *CWPO-C* overexpression affects auxin concentration in Arabidopsis

3-1. Introduction

In Chapter 2, phenotypic observations of *CWPO-C* overexpressed Arabidopsis plants revealed alterations in plant growth and tropism alterations which coincide with the indole-3-acetic acid (IAA) deficient phenotype. The liquid chromatography–tandem mass spectrometry (LC-MS/MS) analyses showed remarkable decrease in IAA content in the transgenic plant. This finding can be explained by the *in vitro* catabolism of IAA by peroxidases (Galston et al. 1953, Hinman and Lang, 1965), and results in this study strongly suggested that CWPO-C contributes to the primary plant growth stage and tropism via IAA catabolism.

3-2. Materials and methods

3-2-1. Histochemical assay

Cell wall lignin was detected in the stem sections of WT and transgenic plants using the Wiesner staining (Adler, 1977). Plants collected at 5-week-old, and 25 μm cross sections were made from the 0.5 cm of the basal parts of stems. The sections were prepared by the cryo-sectioning, and cryo-matrix compound (embedding resin) was removed with water. Sections were stained with1% (w/v) phloroglucinol for 3 min by Wiesner staining as described by Euring et al. (2012). Three biological replicates for each WT and OE11 were used for phloroglucinol staining. At least 2 cross sections per plant were observed by the microscope. Optical microscopic observation was conducted with optical microscopy (Keyence VHX-6000, Osaka, Japan).

3-2-2. *In vitro* reaction of IAA with recombinant CWPO-C and HPLC analysis

Recombinant CWPO-C (rCWPO-C) was prepared and purified according to the described methods by Shigeto et al. (2012). The oxidation of IAA by rCWPO-C was carried out in a 100 mM sodium acetate buffer (pH 5.0) containing 500 µM H_2O_2, 500 µM IAA, 2 U/mL rCWPO-C and rotary-incubated (Rotaflex, Argos) at 10 rpm for 0, 60, 120, 360 min at 25 °C. One U of CWPO-C oxidation activity was defined as the formation of the oxidation product from 2,6-dimethoxyphenol (2,6-DMP) in one µmol/min (Shigeto et al. 2012). As control, the reaction was carried out in the absence of rCWPO-C. Reaction mix was filtered with a Minisart SRP 4 PTFE-membrane and an aliquot of reaction mixture (20 µL) was analyzed by reverse-phase HPLC on a InertSustain AQ-C_{18} column (10 nm, 5 µm, 4.6 × 150 mm; GL Sciences, Japan) using an isocratic elution buffer containing methanol : 1% formic acid mixture (40:60, v/v) at a flow rate of 1.0 mL/min. The eluted products were monitored at the absorbance of 250 nm using a detector (Jasco UV-2070 Plus, Japan).

3-2-3. Endogenous IAA measurements

Stems from 5-week-old plants were harvested, after which 2-cm segments from the tip, middle, and base were frozen in liquid nitrogen and ground to a fine powder. Each ground stem segment was mixed with 5 mL extraction medium (methanol:water:formic acid = 15:4:1, v/v/v) containing 5 ng mL^{-1} deuterium IAA (D_2-IAA) as an internal standard (Kijidani et al. 2014). After 1-h incubation at 4 °C, 5 mL extraction medium was added and the mixture was stirred with a glass rod before incubating for another 1-h at 4 °C. The mixture was centrifuged at 4000 *g* for 10 min and then the supernatant was collected. The supernatant (10 mL) was

purified using the Waters C18 Sep-Pak Cartridge and dried using an evaporator at 60 mmHg and 40 °C. Before loading the supernatant, the cartridge was washed with 5 mL methanol and then equilibrated with 5 mL water adjusted to pH 1.9 with formic acid. The residue dissolved in 4 mL water adjusted to pH 1.9 with formic acid was separated into acidic and basic fractions using the Waters Oasis® MCX Cartridge that was previously washed with 5 mL methanol and then equilibrated with 5 mL water adjusted to pH 1.9 with formic acid. The acidic fraction containing D_2-IAA was eluted using 4 mL methanol. After filtering the eluates using the Acrodisc® Syringe Filter (PTFE, 13 mm, 0.2 μm), they were concentrated to about 300 μL under decompression. The LC-MS/MS analyses were performed using a Dionex Ultimate 3000 UHPLC system (Thermo Fisher Scientific) equipped with the ACQUITY UPLC® BEH C18 column (1.7 μm, 2.1 × 100 mm) and a Q-Exactive mass spectrometer (Thermo Scientific). The mobile phase comprised solvent A (0.1% formic acid–water, v/v) and solvent B (0.1% formic acid–acetonitrile, v/v). The gradient program was as follows: [time (min)/concentration of A (%)/concentration of B (%)] 0/90/10; 7/30/70; 9/10/90; 23/10/90; 26/90/10; and 30/90/10. The flow rate and injection volume were 300 μL min^{-1} and 10 μL, respectively.

3-3. Results

3-3-1. *CWPO-C* overexpression results in a slow stem gravitropic response

Plant growth and development are regulated by plant hormones (Davies, 1995). The observed dwarfism in line OE11 was considered to be related to the plant hormone auxin, which

promotes stem elongation and stimulates growth. Modifications in auxin synthesis adversely affect plant growth, ultimately leading to dwarfism (Cheng et al. 2006). Auxin effects in plants were previously evaluated by examining plant responses to a gravitropic stimulus (Salisbury et al. 1988). In the present study, time taken to reach a 90° stem curvature in OE11, OE12, OE13 and WT Arabidopsis plants were set horizontally was recorded. OE plants bent more slowly and the time required for the stems to bend 90° was almost double that required by WT plants (Table 3-1). In addition, Wiesner staining observations of the cell walls showed very similar between WT and OE11 (Fig. 3-2), suggesting that cell wall and lignification levels may not affect largely to the delay of the bending time in OE11. These results suggest the possibility that *CWPO-C* overexpression modulated the gravitropic response by disrupting auxin accumulation in plant. When *Pcwpo-c*::*GUS* transgenic plants were subjected to the bending test, GUS activity was clearly induced in the bended part of the stem, after 120 min of bending (Fig. 3-1b). While, at zero time of bending test, *Pcwpo-c*::*GUS* transgenic plant expressed typical GUS activity in the apical stem, young leaves and flowers (Figs. 3-1a and 2-1b, g, l respectively), but after 120 min of bending GUS expression in these organs disappeared for unknown reasons. These observations suggest that CWPO-C affects auxin concentration, thereby altering the stem gravitropism response.

3-3-2. Quantification of IAA in Arabidopsis overexpressing CWPO-C

If CWPO-C has an effect on auxin, the auxin content should differ between OE11 and WT plants. According to OE11 results, such higher CWPO-C protein content, shortest stem length and presence of characteristic curled stem phenotype in comparison to OE12 and OE13 lines, we decided to quantify IAA content only in OE11, since it was the most

representative line of CWPO-C effects over IAA related phenotype. Stems from 5-week-old WT and OE11 plants were collected. Regarding line OE11, the straight and curled stems were collected separately. The stems were divided into upper, middle, and lower parts for an analysis of the IAA content (Fig. 3-3). In the stem tip, the IAA content was approximately 10-times lower in OE11 plants than in WT plants. Regarding the other stem segments, the IAA contents in the middle and lower parts were lower in OE11 plants than in WT plants (Fig. 3-3). Furthermore, the IAA content in the curled stem tip of OE11 plants was only about half of that in the straight stem tip of OE11 plants (Fig. 3-3). The dwarfism and curled stem phenotype of OE11 may be attributed to a decrease in IAA contents. The overexpression of *CWPO-C* appears to decrease IAA levels in OE11 plants with or without curled stems. The *in vitro* reaction, in which rCWPO-C reacted and decreased IAA (Fig. 3-4), supported the observed IAA decrease in OE11.

Table 3-1 Bending time of 4-week-old wild-type and OE11-13 Arabidopsis plants

Type	Bending time (min)
Wild-type	86 ± 4.1
OE11	150 ± 3.5
OE12	152 ± 4.1
OE13	132 ± 14.4

Note: Bending time refers to the time required for the horizontally placed stem to bend 90°. Four biological replicates were analyzed and the data are presented as the mean ± standard deviation. OE11-13: *CWPO-C*-overexpressing line 11-13

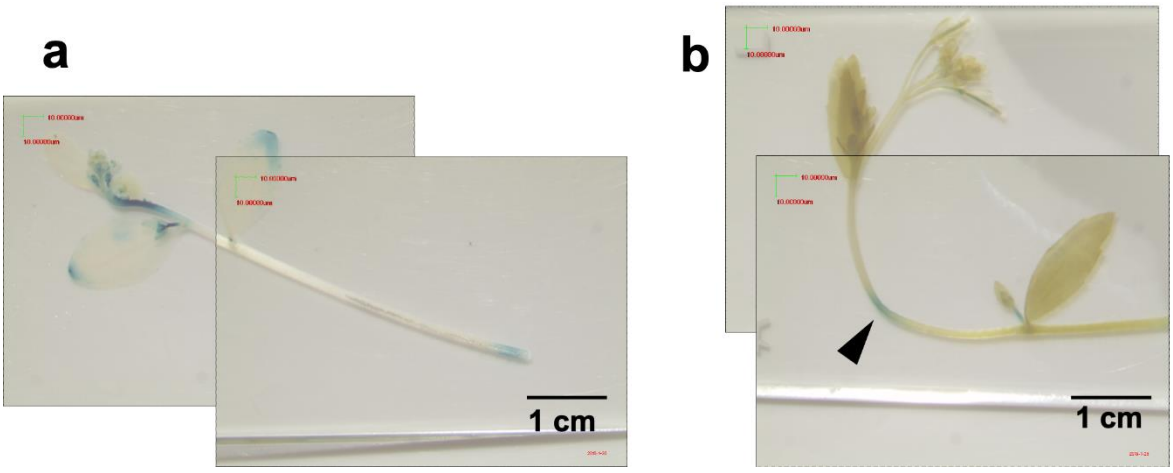

Fig. 3-1 Gravitropic response of the *CWPO-C* promoter in transgenic Arabidopsis plants carrying the *Pcwpo-c*::*GUS* construct. **a** Transgenic plant before bending (control). **b** Transgenic plant analyzed by GUS staining after bending for 120 min. The GUS signal was detected at the bent part of the stem (black arrow)

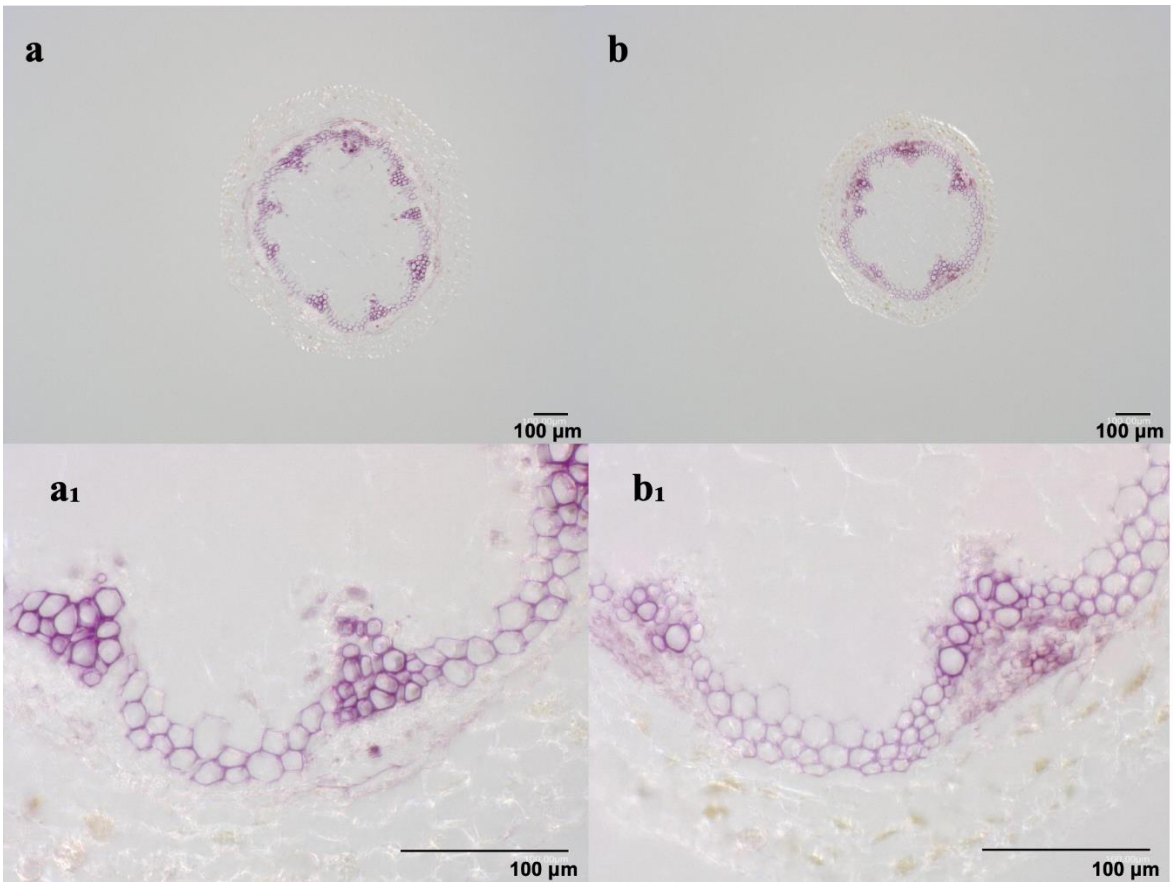

Fig. 3-2 Wiesner staining of 5-week-old Arabidopsis basal stem. **a-a₁** WT, **b-b₁** OE11

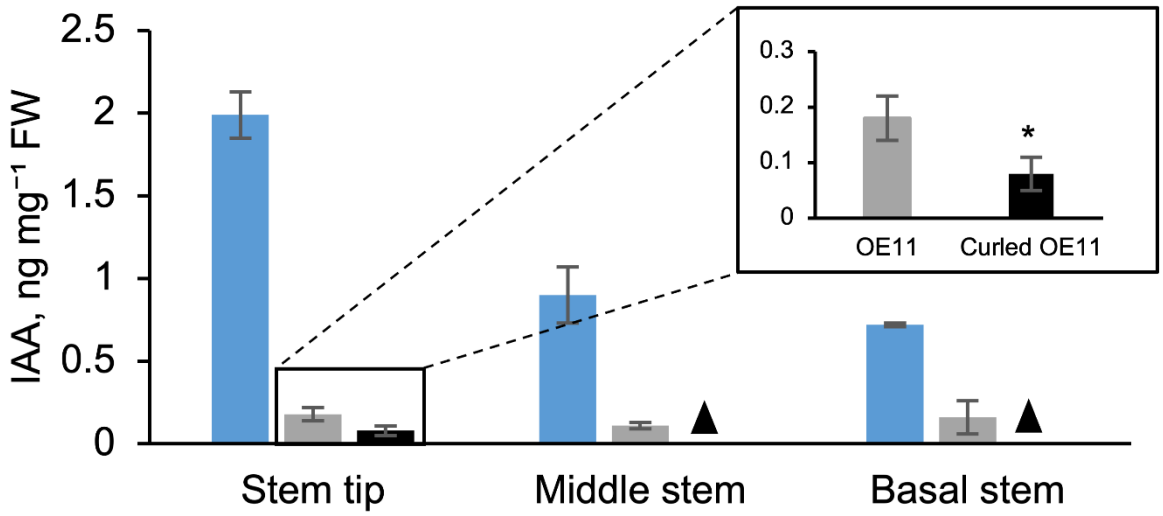

Fig. 3-3 Analysis of the indole-3-acetic acid (IAA) content in the stems of 5-week-old WT (blue), OE11 (gray), and curled OE11 (black) plants. Data are presented as the mean ± standard deviation. Three biological replicates were analyzed. *: Significant difference ($p < 0.05$) relative to the OE11 stem tip (Student's *t* test). ▲: IAA contents in the middle and basal parts of the curled stem were not determined because the samples were too small

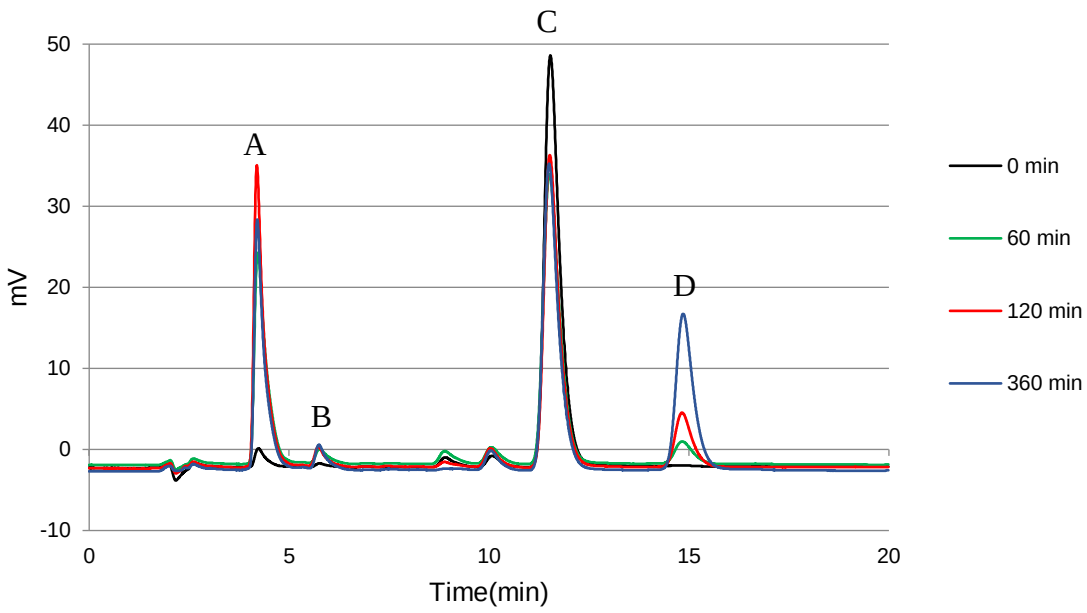

Fig. 3-4 Elution profiles of the oxidative products of IAA by recombinant CWPO-C. The HPLC chromatograms at the reaction time 0, 60, 120, 360 min were shown. A: 4.24 min product peak, B: 5.75 min oxIAA peak, C: 11.53 min IAA peak and D: 14.86 min product peak. The reaction products were analyzed on the reverse-phase HPLC with a AQ-C_{18} InertSustain column. The eluted products were monitored at O.D. 250 nm

3-4. Discussion

Gravitropism causes stems to bend because of the associated change in auxin distribution. The time required for a stem placed horizontally to bend 90° was used as a simple index, but sensitive assay, for investigating whether auxin is involved in the stem curvature observed in CWPO-C OE plants. A significant delay in the bending of the OE11, OE12 and OE13 stem (Table 3-1) suggests that CWPO-C interferes with the plant cell elongation mechanism. Regarding the gravitropic response, OE11 and WT showed similar cell wall lignin in the Wiesner staining (Fig. 3-2), which let us deduce that the delay in bending time of OE11 was not due to changes in the cell wall lignin. Rakusová et al. (2011) observed that inhibiting the auxin transporter PIN3 leads to decreased auxin mobilization during gravitropism, which results in delayed bending and a smaller curvature. In another study, Gutjahr et al. (2005) demonstrated that an IAA treatment increases the curvature angle and accelerates the bending of rice hypocotyls. The inhibition of stem bending in the current study may be explained by the inactivation of auxin through the oxidation by CWPO-C. Furthermore, the disrupted IAA distribution due to an excess of CWPO-C is a plausible explanation for the aforementioned curled stem tip of OE11 plants. It is also possible that the stem curvature in OE11 plants was the result of Prx-derived •OH radicals exhibiting an auxin-like effect. Peroxidases help strengthen cell walls via lignification, but they can also weaken cell walls and promote cell elongation, with the Prx-derived •OH inducing the oxidative cleavage of cell wall polysaccharides (Liszkay et al. 2003, Kunieda et al. 2013).

In this study, OE11 plants had decreased IAA contents (Fig. 3-3). Moreover, the severely curled OE11 stem tips contained more CWPO-C and significantly less IAA than the straight OE11 stem tips (Table 2-2, Fig. 3-3 respectively). The observations described only on OE11 line still have a low possibility that IAA decrease can be due to the insertion site of the transgene but not the peroxidase itself. On the other hand, the similar phenotype such the reduced stem length and bending time, observed in all three lines (OE11, OE12 and OE13), might be due to the peroxidase expression. This suggests that CWPO-C catabolizes IAA in plants. The reaction of IAA with Class III Prxs, such as horseradish Prx, were first demonstrated under *in vitro* conditions (Galston et al. 1953). The PxB2 Prx from *Vitis vinifera* roots was reported to have oxidase activity toward IAA (Vatulescu et al. 2004). In a preliminary assay, rCWPO-C reacted with IAA *in vitro*, the results showed 2 unidentified oxidative products of IAA, demonstrating the oxidative activity of rCWPO-C towards IAA (Fig. 3-4). We had also confirmed that two major products are not 2-oxindole-3-acetic acid (oxIAA) in the rCWPO-C - IAA *in vitro* reaction (Fig. 3-4). It seems that IAA oxidation by rCWPO-C differs from previous reported oxidation pathway, where oxIAA is the major oxidation product. There have been reports describing the Prxs in IAA reaction *in vitro*; however, the available information regarding Prx-catalyzed IAA *in planta* is very limited. It has been well-known that some peroxidases expression could be affected by other peroxidases (Cosio et al. 2009), therefore, it is difficult to attribute the peroxidase activity changes only to the overexpression of the peroxidase introduced. For this reason, we focused on the effect of *CWPO-C* overexpression to the phenotype in this study. Previously, Cosio et al. (2009) proved that the heterologous expression of *CpPrx01* from *Cucurbita pepo* in

Arabidopsis lengthens the roots and hypocotyls and decrease the IAA levels. In contrast, the OE11 plants in this study had shortened stems (Fig. 2-2b) and decreased IAA levels (Fig. 3-3), which is similar to the auxin-deficient phenotype of Arabidopsis mutants in which multiple *YUC* genes are silenced (Cheng et al. 2006, Chen et al. 2014), however, there have been no report that described the direct relation between peroxidase and *YUC* expression, so far. The results of the earlier study by Cosio et al. (2009) are not inconsistent with our findings because auxin effects on cell elongation (i.e., promotion or suppression) depend on the concentration and the organ (Tanaka et al. 2006, Vanneste and Friml, 2009). In fact, compared with the WT plants, the OE11, OE12, OE13 lines had shorter stems, but longer roots (Table 2-3).

3-5. SUMMARY

In this chapter, results demonstrated that the overexpression of *CWPO-C*, which encodes a class III peroxidase, decreased the IAA content in Arabidopsis and results in the phenotype that is consistent with the typical phenotype due to the auxin deficiency. This strongly suggests that CWPO-C participates in the regulation of plant growth and decrease IAA concentration. Furthermore, CWPO-C may play a role in the cell elongation, rather than controlling the initiation of these processes *via* auxin.

In the next chapter, in order to estimate the *in vivo* function of CWPO-C without using the model plant Arabidopsis, the transcription of *CWPO-C* gene was analyzed in several organs,

and the localization of *CWPO-C* promoter was investigated in the plant species where CWPO-C was isolated, *Populus alba*.

Chapter 4: *CWPO-C* expression through plant growth and lignification tissues in Poplar

4-1. Introduction

Class III plant peroxidases are encoded by a large gene family, and poplar (*Populus trichocarpa*) contains 93 genes (Ren et al. 2014). The peroxidases differ in their individual substrate oxidation activities and physiological roles (Shigeto et al. 2016). While the roles of peroxidases in various processes, such as lignification (Shigeto et al. 2016, Hoffmann et al. 2020), plant defense (Almagro et al. 2009), development (Cosio et al. 2009, Müller et al. 2009), germination Müller et al. 2009, (Kunieda et al. 2013, Jemmat et al. 2020), and seed longevity (Renard et al. 2020) have been reported, to date, relatively few peroxidases have been functionally annotated, and the *in vivo* function of most peroxidases remains unclear.

Previously, *CWPO-C* promoter analysis in Arabidopsis using β-glucuronidase (*GUS)* as a reporter gene revealed that it was strongly expressed in immature tissues, regardless of the organ (Yoshikay-Benitez et al. 2022). We also reported that transgenic Arabidopsis plants overexpressing *CWPO-C* exhibited suppression of stem elongation and seed development with an unexpected phenotype: stem tip curled in overexpressing plants was about 60% of that in the wild type (Yoshikay-Benitez et al. 2022). These results, using a heterologous *CWPO-C* expression system, suggested that *CWPO-C* is involved in plant organ development or early growth. Other reports using heterologous peroxidase expression suggested that peroxidases are involved in plant development and growth. Overexpression of peroxidase *CpPrx01* in *A. thaliana* enhanced stem growth (Cosio et al. 2009). Overexpressed *HRP-C1a* in *Nicotiana tabacum* and hybrid poplar resulted in faster growth and longer stems (Kawaoka et al. 1994, Kawaoka et al. 2003). Plant growth and organ

development are regulated *via* extremely complex networks involving molecules such as phytohormones.

Heterologous expression using Arabidopsis has the advantage that it can be analyzed throughout one generation in approximately 3 months; however, there are some cases where its expression pattern differs from poplar, which might be because of differences in the properties of the transcription regulating factors. A further limitation is that a reverse genetic strategy for the suppression of the targeting *CWPO-C* gene is not available in the heterologous expression system, since Arabidopsis does not possess *CWPO-C* gene in its genome. In this study, we prepared and analyzed transgenic poplar plants to confirm the expression pattern of *CWPO-C* and to investigate the role of CWPO-C in poplar development, growth and lignification using overexpression and suppression of *CWPO-C*.

4-2. Materials and Methods

4-2-1. Generation of transgenic plants

Preparation and construction of plasmids for GUS assays and *CWPO-C*-overexpression were as described by Yoshikay-Benitez et al. (2022). Both, the CWPO-C overexpression and suppression (RNAi) constructs were driven by the Cauliflower Mosaic Virus 35S promoter (CaMV 35S). For construction of the RNAi silencing vector, a hairpin-type gene cassette including a 432-bp fragment of *CWPO-C* open reading frame from nucleotides 633 to 1064 (relative to the ATG start codon) was connected between *Bam*HI and *Sac*I sites of pBF2.

Transformation of poplar was performed as described by Takata and Eriksson (2012), Song et al. (2019) and Nanasato et al. (2015) with some modifications. Briefly, stems from wild-type *Populus alba* were excised (1 cm length), and *Agrobacterium tumefaciens* strain LBA4404 carrying the binary vector as above was used to transfect explants. Explants were transfected in Murashige–Skoog (MS) medium, pH 5.6, x1 MS vitamins, 3% (w/v) sucrose, *A. tumefaciens* at OD_{600} = 0.4–0.9, 20 µM acetosyringone and 0.015% Silwet L-77 for 1 hour with shaking at 60 rpm. Co-cultivation of explants was performed in the dark for 3 days in MS medium, pH 5.6, 0.3% Gelrite and three layers of filter paper N^{O}. 2 pre-wetted with 5 µM acetosyringone in liquid MS medium. After co-cultivation, the explants were washed twice with sterile water and once with MS medium, pH 5.6, with 1× MS vitamins, 3% sucrose and 50 mg/L meropenem. Finally, explants were blotted on filter paper and transferred to MS medium, pH 5.6, 1× MS vitamins, 3% (w/v) sucrose, 0.3% Gelrite, 0.2 mg/L 6-benzyl amino purine (BAP), 0.1 mg/L indole-3-butyric acid (IBA), 0.01 mg/L thidiazuron (TDZ), 50 mg/L kanamycin and 50 mg/L meropenem. The culture medium was renewed every 3 weeks. Callus formation was observed after 3–6 weeks. For induction of multiple shoots, callus was transferred onto 0.3% Gelrite-solidified MS medium, pH 5.6, with 1× MS vitamins, 3% (w/v) sucrose, 0.2 mg/L BAP and 0.01 mg/L TDZ, and was cultured in a growth chamber (CLE-303; TOMY SEIKO Co., Ltd., Tokyo, Japan) at 25±1ºC under 16 h light (65 µmol photons $m^{-2}s^{-1}$ from cool-white fluorescent tubes) and 8 h dark.

4-2-2. Plant materials and growth conditions

Populus alba wild type and transgenic plants were cultured on 0.3% Gelrite-solidified MS medium, pH 5.6, with 1× MS vitamins and 3% (w/v) sucrose, 50 mg/L kanamycin (only for transgenic plants) in plant boxes. They were incubated in the growth chamber, as above.

4-2-3. Preparation of stem cryosections

For cryostat sectioning, stem pieces 5 mm in length were vacuum-incubated with 30% sucrose for 10 min, immersed in the mixture of Cryomatrix (Thermo scientific, USA) and 30% sucrose (1:1) for 10 min, then incubated in Cryomatrix for 10 min. Finally, Cryomatrix-embedded sections were mounted in a plastic cryomold (Tissue-Tek, The Netherlands), snap-frozen in liquid nitrogen, and stored at −80°C. Sections of the stem were cut with a cryostat (Thermo Scientific HM 525 Cryostat, VWR International, PA, USA) at −15°C, and mounted on glass slides for histochemical staining or on PEN-membrane 2.0-µm glass slides (Leica, Germany) for RNA extraction. Prior to laser micro-dissection, the 25-µm sections were fixed in cold RNase-free 99.5 % ethanol at −20°C for 10 sec, washed of Cryomatrix compound with RNase-free water for 2 min, and refixed in cold RNase-free 99.5% ethanol at −20°C for 1 min. All instruments and reagents were treated to make RNase-free to avoid RNA degradation.

4-2-4. Laser micro-dissection of stem cryosections

Sections mounted on PEN glass slides were air-dried and micro-dissected with a laser micro-dissection (LMD) microscope (LMD7, Leica Microsystems CMS GmbH, Wetzlar, Germany) at room temperature. The LMD technique was combined with RNA isolation and transcript analysis by real-time quantitative PCR (RT-qPCR). LMD was performed as

described by Abbot et al. (2010) with adaptations for the cell and tissue types used. For optimal dissection we used the maximum laser intensity and the slowest cutting speed. Different micro-dissected tissues were collected individually into the cap of nuclease-free 0.5-mL PCR tubes (Axygen, Union City, CA, USA) containing 60 μL lysis buffer supplied with the RNAqueous-Micro RNA Kit (Ambion, Inc., Austin, TX, USA). The collected dissection samples were kept in liquid nitrogen until they were subjected to RNA extraction.

4-2-5. RNA extraction and real-time PCR

Total RNA from micro-dissected tissues was isolated using the RNAqueous-Micro RNA Kit (Ambion, Inc., Austin, TX, USA). The RNA was treated with DNase I inactivation reagent supplied with the kit. First-strand cDNA was synthesized using ReverTra Ace® (Toyobo Co.). The cDNA solution was used as template for PCR. The primer sequences for the *CWPO-C* gene were:

CWPO-C-left (GCTCGTGATTCTGTTGTTTTGACAAAG),

CWPO-C-right (GCTGCAAACTTCTGTTTCTGCAC)

and for the reference gene

UBQ (BU879229): *UBQ*-left (TTCACTTGGTGCTGCGTCTC),

UBQ-right (TCTGAGCTCTCGACCTCCAG).

The copy numbers of the fragments for each target gene were estimated as described by Takeuchi et al. (2018) with adaptations for the tissue types used. The relative quantity of the target mRNA was normalized using *UBQ* gene as an internal standard.

4-2-6. Western blot analysis

Western blot was done as described by Yoshikay-Benitez et al. (2022) using an anti-CWPO-C antibody and the anti-rabbit IgG secondary antibody conjugated with horseradish peroxidase (Proteintech Group Inc.) at a dilution of 1:250 (v/v) and 1:500 (v/v) in 1× PBS (pH 7.4), respectively. Briefly, a 15-μg protein sample was separated by 10% (w/v) SDS-polyacrylamide gel electrophoresis and then electroblotted onto a PVDF membrane (Merck Millipore Ltd., Tullagreen, Ireland). PVDF membranes were blocked overnight using 5% (w/v) skimmed milk dissolved in 1× PBS buffer. Membranes were blotted with the antibody then washed twice in 1× PBS and probed with a goat anti-rabbit IgG horseradish peroxidase conjugate (Proteintech Group Inc.). After washing the membrane twice in 1× PBS, the immunopositive bands were visualized using WSE-7140 EzWestBlue W (ATTO). Other 15-μg protein samples were separated by electrophoresis and stained with Coomassie Brilliant Blue (CBB) to detect Rubisco.

4-2-7. GUS staining

GUS staining of transgenic poplar bearing *Pcwpo-c*::*GUS* was done as described by Vitha et al. (1993). Briefly, transgenic poplar organs were incubated with 0.5% paraformaldehyde for 45 min at −0.07 MPa vacuum to infiltrate the fixation agent. Then, after washing twice in 100 mM phosphate buffer (pH 7), the samples were transferred to GUS staining solution containing 100 mM $NaPO_4$, 0.5 mg/mL x-gluc (5-bromo-4-chloro-3-indolyl-β-D-glucuronide), 0.2 mM $K_3Fe(CN)_6$, 0.2 mM $K_4Fe(CN)_6$, pH 7, and incubated overnight. Subsequently, samples were post-fixed in 60% ethanol, 5% acetic acid, 3.7% formaldehyde

solution for 2 h. Finally, samples were dehydrated with an ethanol concentration gradient (70%, 80%, 90%, 100%) for 1 h each and chloral hydrate/water/glycerol (25:9:3, w/w) solution overnight to clear the tissues.

4-3. Results

4-3-1. *CWPO-C* is expressed in meristematic and developing tissues

Transgenic poplar with the construct expressing the *GUS* gene under the control of the *CWPO-C* promoter (*Pcwpo-c*::*GUS*) was analyzed. GUS assays showed that *Pcwpo-c*::*GUS* transgene was expressed in stem, leaves and roots (Fig. 4-1a). The upper and middle stem had potent GUS activity (Fig. 4-1a). The whole of young leaves at the upper stem were GUS stained, and the staining in the leaves tended to fade when the leaf turned older (Fig. 4-1a). Arabidopsis bearing *Pcwpo-c*::*GUS* also showed strong expression in young leaves (Yoshikay-Benitez et al. 2022). Interestingly, *Pcwpo-c*::*GUS* was expressed in shoot tips (Fig. 4-1b1) and the base of axillary buds (Fig. 4-1c1), although our previous studies suggested that CWPO-C protein expression was related to lignin polymerization. Microscopic observation revealed that *CWPO-C* was preferentially expressed in meristematic tissues, the shoot apex and axillary meristems (Fig. 4-1b2, c2). Also, Fig. 4-1d1, d2 shows GUS staining in the developing xylem of the middle stem. To complement the visual expression patterns of *Pcwpo-c*::*GUS*, we applied RT-qPCR analysis to plant organs where GUS activity was observed: we found *CWPO-C* was more highly expressed in the middle stem than in the shoot tip and other stem parts (Fig. 4-2).

The *CWPO-C* promoter was preferentially expressed in the shoot tip (Fig. 4-1b1, b2). The transcript abundance of *CWPO-C* in the shoot tip was further examined by RT-qPCR analysis combined with LMD. As shown in Fig. 4-3, *CWPO-C* was strongly expressed in the shoot apex (Fig. 4-3d). In contrast, *CWPO-C* showed lower expression in the stem cambium (Fig. 4-3d). Results showing high *CWPO-C* expression as determined by RT-qPCR were consistent with the GUS staining observations (Fig. 4-3b, c). The meristems are responsible for the growth and development of tissues, and the specific expression of *CWPO-C* in meristematic tissues, such as shoot apex and axillary meristems, indicates that CWPO-C might exert a substantive biological function in plant growth and development.

Considering these results, and also our previous report using heterologous expression system in Arabidopsis showing that *CWPO-C* promoter activity was observed in any immature organs including leaf, stem, root, flower and fruit, it can be assumed that CWPO-C is involved in development or differentiation or early growth of each organ (Yoshikay-Benitez et al. 2022). If that were the case, *CWPO-C* would be expected to express strongly in newly generating axillary branches. The presence of the shoot apex inhibits axillary bud outgrowth in the phenomenon called apical dominance. Decapitation of the shoot tip releases the axillary buds from growth inhibition. As expected, in transgenic poplar bearing *Pcwpo-c*::*GUS*, when the tip of the main stem was cut, staining for GUS activity beneath the stem tip disappeared, and strong staining was observed in the newly developed axillary branches (Fig. 4-4a). In other experiments, using callus in which multiple adventitious buds were induced, similarly, strong GUS staining was observed in the adventitious buds derived from the callus (Fig. 4-4b). These observations strongly support the hypothesis that CWPO-C

participates in plant growth and development, and specifically organogenesis at the shoot apex and axillary buds.

4-3-2. *CWPO-C* overexpression modifies growth rates

To assess the functional role of CWPO-C during poplar growth and development, we generated three independent CWPO-C overexpression (OE) lines and two independent RNAi lines. Six-week-old plants were analyzed for gene expression by RT-qPCR (Fig. 4-5a, b) and protein expression by western blot using an anti-CWPO-C antibody (Fig. 4-5c, d). Compared with WT, the expression of *CWPO-C* transcripts were quantified as 17, 19 and 12-fold higher in OE1, OE2 and OE4, respectively (Fig. 4-5a). The two RNAi lines, RNAi1 and RNAi2, showed approximately 85% and 99% lower *CWPO-C* expression, respectively, compared with WT (Fig. 4-5b). Expressed CWPO-C protein were clearly higher in all OE lines (Fig. 4-5c). CWPO-C protein was not detectable in the RNAi lines, nor in WT (Fig. 4-5c, d). Considering both transcript and protein analyses, CWPO-C was evidently up-regulated in the three OE lines and was well suppressed in the two RNAi lines.

The stem growth rate of *CWPO-C* overexpression lines OE1, OE2, OE4 was higher compared with WT (Fig. 4-8b). In contrast, the growth rates of *CWPO-C* RNAi1 and RNAi2 were not significantly different from WT (Fig. 4-8a).

Leaves of transgenic line OE1 showed shorter leaves size with dark green color, while line RNAi1 had larger leaves size with light green color (Fig. 4-10).

The impact of CWPO-C overexpression or suppression on vascular development in the stem was observed in basal stem cross-sections (Fig. 4-6a1–3; Fig. 4-9a1–4). In contrast to stem

elongation, stem cross-sectional area significantly increased in RNAi1 and RNAi2 (Fig. 4-6a2; Fig. 4-9a2; Fig. 4-7a). This increase was mainly the result of enlargement of the cortical area (Fig. 4-6a, b; Fig. 4-9a, b), and consequently the proportion of xylem in the cross-section decreased (Fig. 4-7b). The enhancement of the cortical area in the stem seems to be a positive effect for the plant growth in response to the decreased proportion of xylem in the cross-section (Fig. 4-6, 4-7). The decrease of xylem area is a negative effect of the CWPO-C suppression in RNAi lines. The mechanism of xylem area affected by the lower presence of CWPO-C is unknown._These results suggest that CWPO-C promoted vertical growth and differentiation of xylem, while not affecting horizontal growth.

Table 4-1 Expression sites of *CWPO-C* in WT poplar and Arabidopsis

organ/plant	P. alba	3-day-old A. thaliana	3-week-old *A. thaliana*	5-week-old *A. thaliana*
stem meristem	shoot apex	shoot apex	shoot apex	shoot apex
upper stem	xylem	n.a.	n.t.	xylem
middle/lower stem	xylem, cortex, petiole base	n.a.	n.t.	cortex around cauline leaf base
petiole	entirely	n.a.	n.d.	entirely
root	entirely except the tip	entirely except the tip	entirely except the tip	n.t.
flower	n.a.	n.a.	n.t.	flower bud
fruit	n.a.	n.a.	n.a.	inmature siliques and seeds
upper leaves	entirely	n.a.	entirely, hydathodes	n.t.
middle/lower leaves	tip, hydathodes, trichome, stomata	n.a.	tip, hydathodes	tip, hydathodes
axillary bud	entirely	n.a.	n.t.	entirely
cotyledon	n.a.	tip, trichome, stomata	n.a.	n.a.
hypocotyl	n.a.	around cotyledon and root base	n.a.	n.a.

n.t.: not tested; n.a.: not applicable; n.d.: not detected. Arabidopsis data in Yoshikay-Benitez et al. (16).

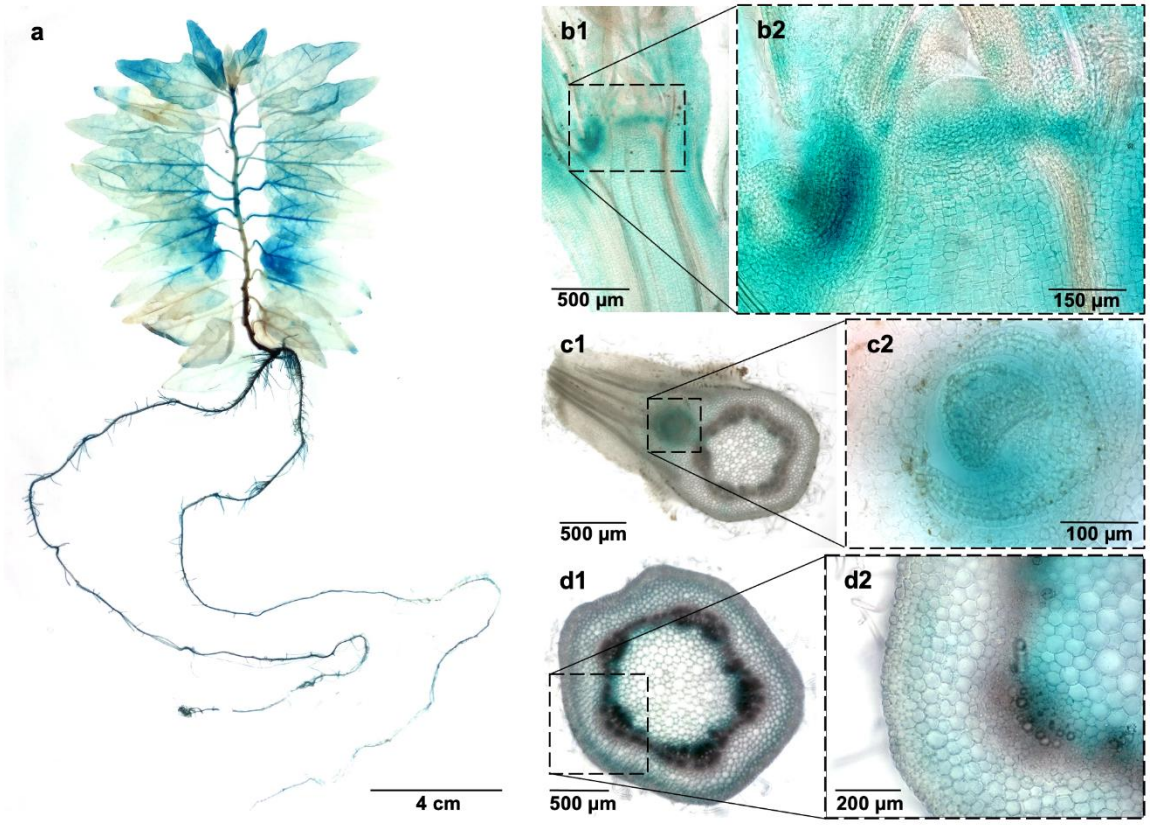

Fig. 4-1 *CWPO-C* promoter analyses in poplar using *GUS* reporter gene. **a** Whole 6-week-old plant. **b1** Longitudinal section of shoot tip, **b2** Longitudinal section of shoot apex. **c1** Cross-section of axillary bud, **c2** Cross-section of axillary meristem. **d1** and **d2** Cross-section of developing xylem in the middle stem

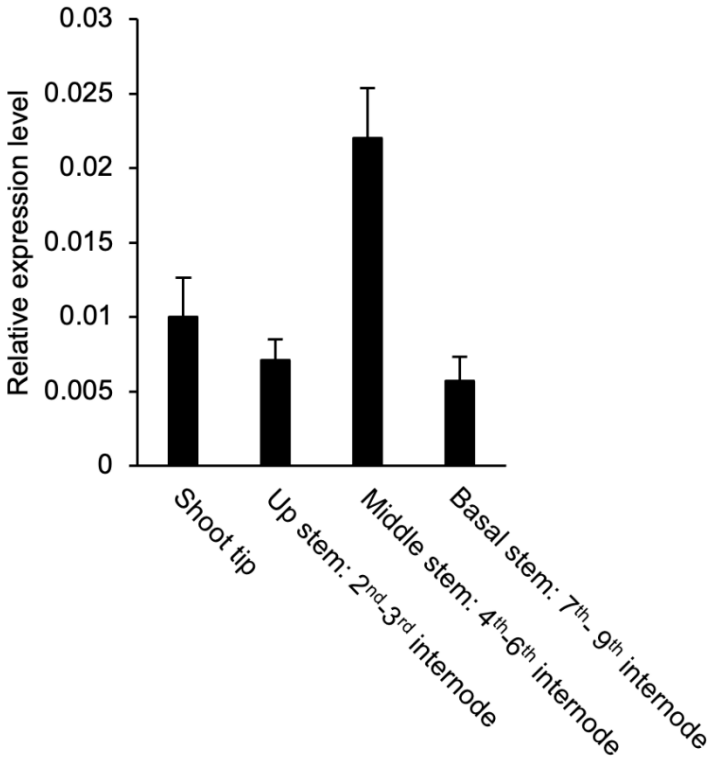

Fig. 4-2 Relative expression of *CWPO-C* gene in different parts of the stem in 6-week-old WT poplar. Analyses were conducted with three biological replicates (mean ± standard deviation). Data are presented as relative transcript abundance normalized to *UBQ* expression

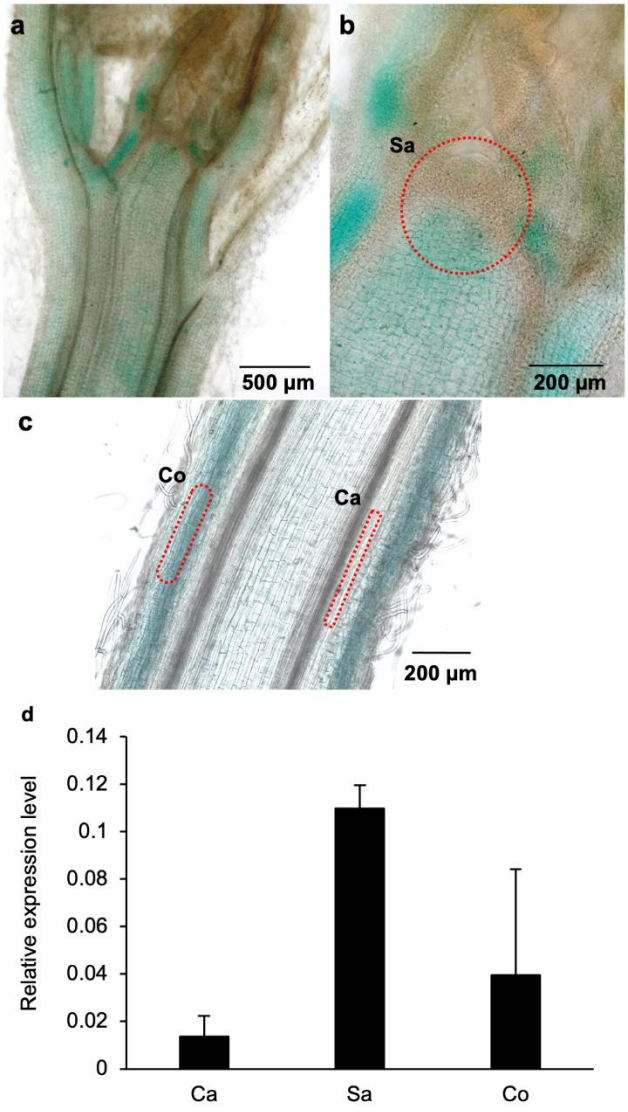

Fig. 4-3 Localization of *CWPO-C* transcripts**. a–c** Localization of GUS activity in longitudinal sections**. a, b** Stem tip. **c** Middle stem. **d** Gene expression of *CWPO-C* by RT-qPCR combined with laser micro-dissection. Ca: cambium tissues, Sa: shoot apex, Co: collenchyma. Data are presented as relative transcript abundance normalized to *UBQ* expression and mean with standard deviation of triplicate analyses

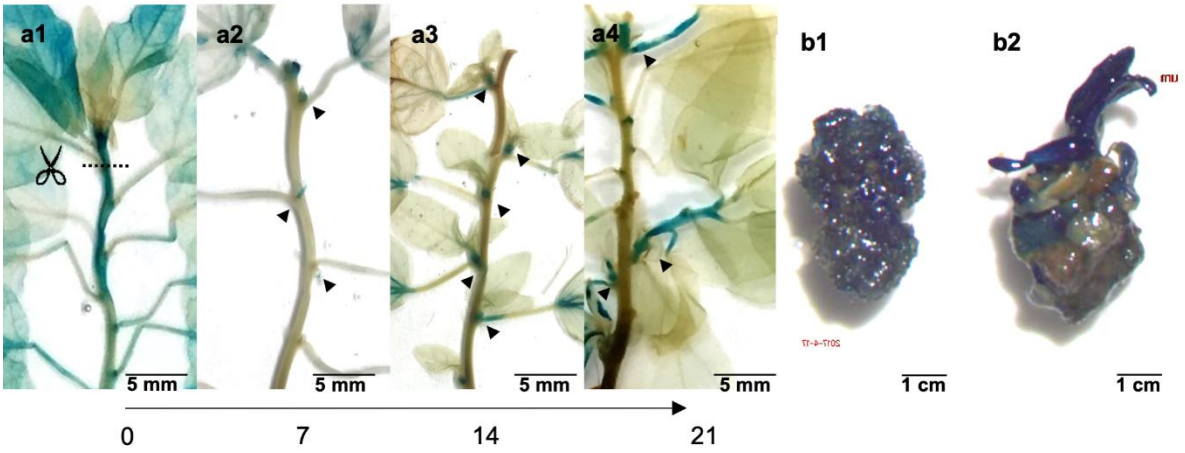

Fig. 4-4 *Pcwpo-c*::*GUS* expression during axillary bud outgrowth and adventitious bud induction. **a1**–**a4** Axillary bud outgrowth induction. **a1** Before stem tip decapitation (dotted line indicates decapitation position). **a2**–**a4** Sequence of axillary bud outgrowth (7, 14 and 21 d after decapitation, respectively). Black arrows indicate newly generated buds in the stem. **b1** Callus. **b2** Adventitious bud outgrowth on callus

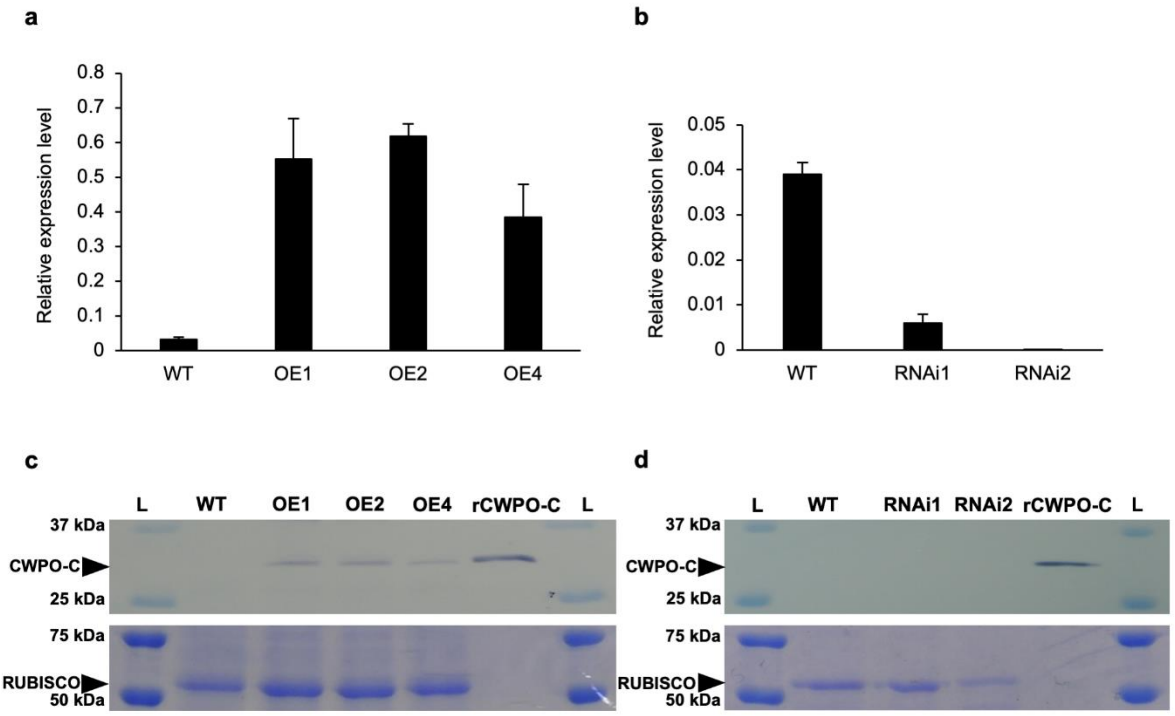

Fig. 4-5 Expression of *CWPO-C* and CWPO-C protein in transgenic poplar lines. **a, b** *CWPO-C* expression levels in 6-week-old overexpression (OE) and suppression (RNAi) transgenic poplar lines. **a** *CWPO-C* expression in WT and three OE lines. **b** *CWPO-C* expression in WT and two RNAi lines. Relative expression levels (mean ± standard deviation) measured by RT-qPCR were calculated from three biological replicates. Data are presented as relative transcript abundance normalized to *UBQ* expression. **c, d** Western blot analysis of CWPO-C protein in transgenic lines using an anti-CWPO-C antibody. **c** WT and three OE lines. **d** WT and two RNAi lines. Upper panels: recombinant CWPO-C protein as a standard marker (rCWPO-C, arrow). Lower panels: proteins stained with Coomassie brilliant blue; arrow indicates Rubisco. L: Molecular weight markers

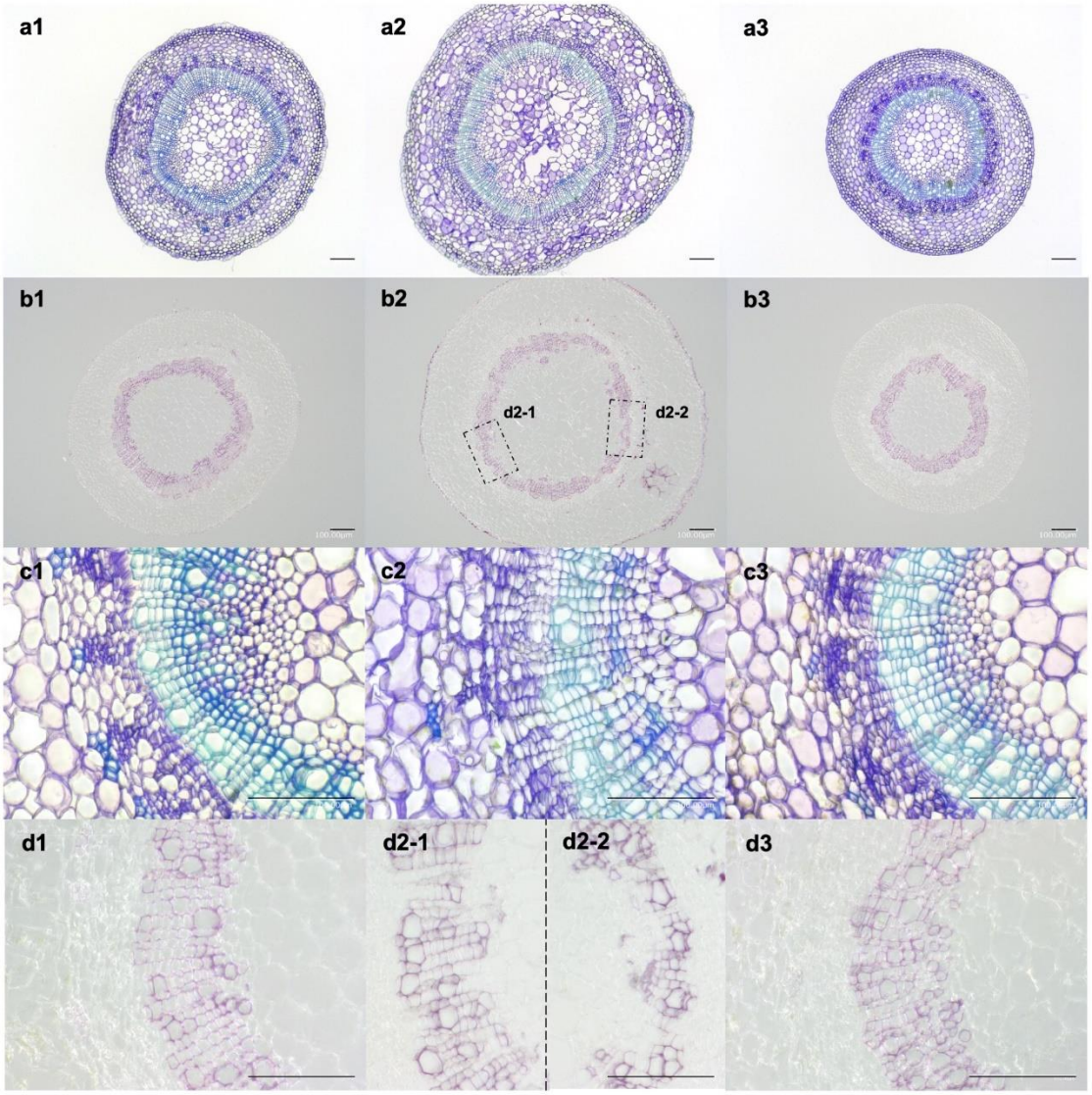

Fig. 4-6 Cross-sections of basal stem of CWPO-C transgenic poplar lines. **a, c** Toluidine blue staining. **b, d** Wiesner staining. **a1, b1, c1, d1** WT. **a2, b2, c2, d2** RNAi suppression line RNAi1. **a3, b3, c3, d3** Overexpression line OE1. Sections (20 μm thick) were prepared from the basal stem of 6-week-old plants. Bar 100 μm

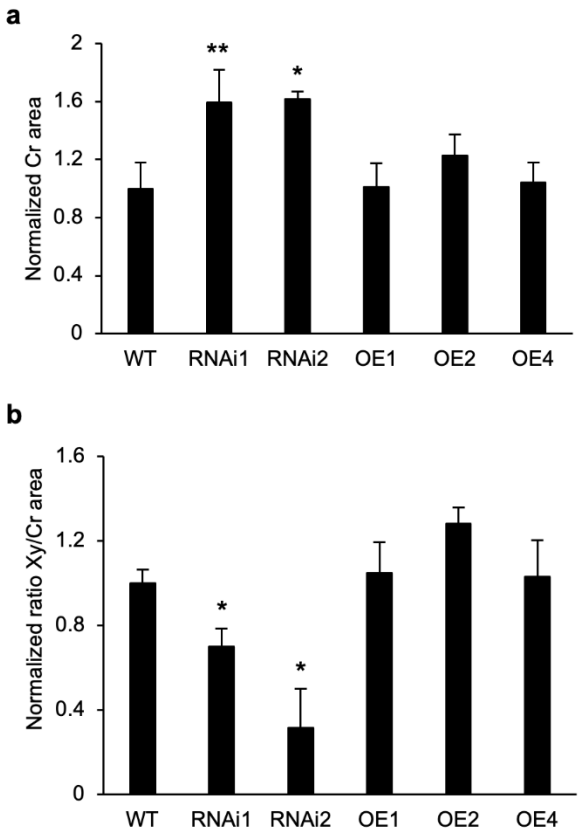

Fig. 4-7 Effect of CWPO-C expression on stem and xylem formation in transgenic poplar. **a** Cross-sectional (Cr) area of whole basal stem. **b** Ratio of xylem/whole cross-sectional (Xy/Cr) area. Data are presented relative to the WT, which was set to 1. Mean ± standard deviation of four biological replicates. *: Significant difference ($p < 0.05$), **: significant difference ($p < 0.01$) compared with WT (Student's *t* test). OE1, OE2 and OE4: CWPO-C OE line 1, 2 and 4. RNAi1 and RNAi2: CWPO-C RNAi line 1 and 2

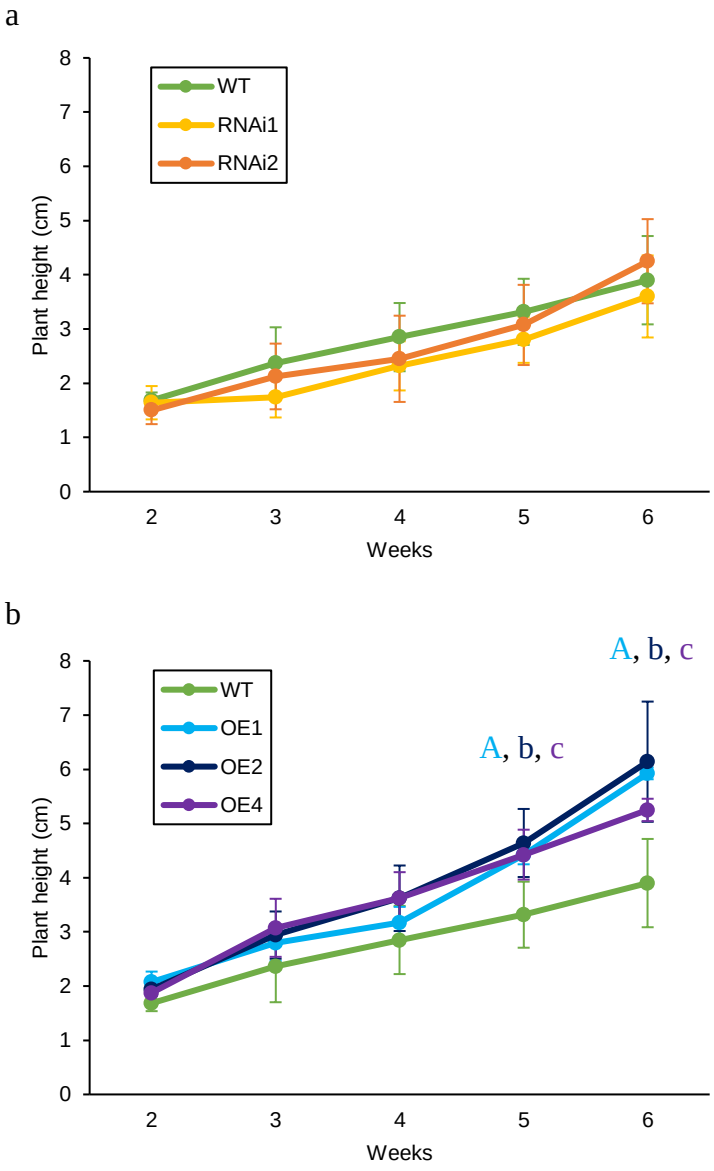

Fig. 4-8 Effect of CWPO-C expression on stem growth in CWPO-C transgenic lines. **a** RNAi suppression lines 1 and 2. **b** Overexpression lines OE1, 2 and 4. Different letters represent significant differences. Lower-case letter: significant difference ($p < 0.05$), upper-case letter: significant difference ($p < 0.01$) compared with WT (Student's *t* test). Four biological replicates were analyzed, and data are presented as the mean ± standard deviation

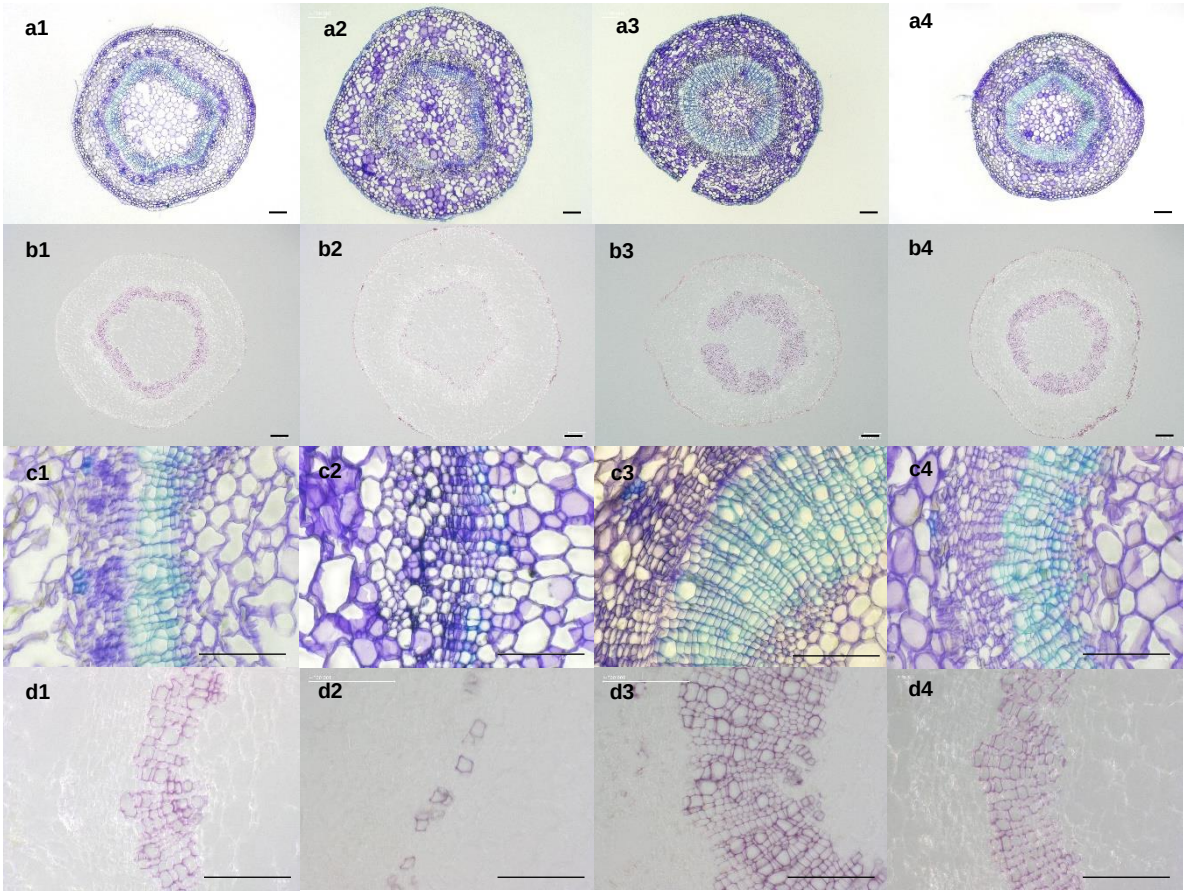

Fig. 4-9 Cross-sections of basal stem of CWPO-C transgenic poplar lines. **a, c** Toluidine blue staining. **b, d** Wiesner staining. **a1, b1, c1, d1** WT**. a2, b2, c2, d2** RNAi suppression line RNAi2. **a3, b3, c3, d3** Overexpression line OE2. **a4, b4, c4, d4** Overexpression line OE4. Sections (20 μm thick) were prepared from the basal stem of 6-week-old plants. Bar 100 μm

a

b

Fig. 4-10 Leaf phenotype in CWPO-C transgenic poplar lines. **a** Leaf color and border shape. Left to right: WT, OE1 and RNAi1. **b** Leaves in 6-week-old poplar. Left to right: younger to older leaves. Upper row: WT; middle row: OE1; lower row: RNAi1

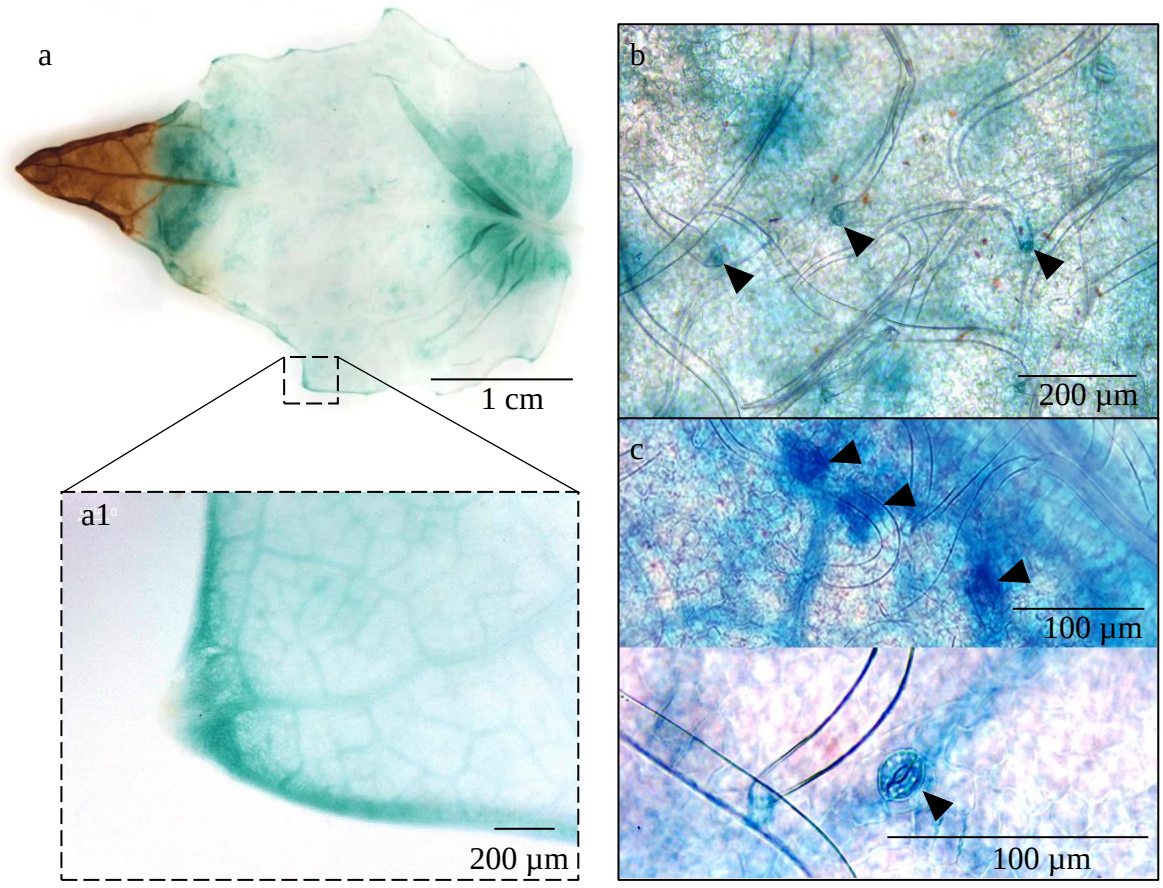

Fig. 4-11 *GUS* expression driven by *CWPO-C* promoter in poplar leaf. **a** Leaf. **a1** Hydathode. **b** Trichome (black arrows: base of trichome). **c** Stomata (black arrow: stoma)

4-4. Discussion

CWPO-C has been considered to be specifically involved in the lignification process of cell walls, since our previous research indicated that CWPO-C has a unique oxidative activity towards monolignols and lignin polymer (Aoyama et al. 2002, Sasaki et al. 2004). However, our recent findings showed that *CWPO-C* was expressed in immature tissues, such apical meristem, young upper stems, developing xylem and young leaves in *Arabidopsis thaliana* transformed with *Pcwpo-c*::*GUS* (Yoshikay-Benitez et al. 2022). In the current study, our results using poplar with the same *Pcwpo-c*::*GUS* construct indicated similar characteristic expression sites of *CWPO-C*, namely the upper stem, developing stem xylem and cortex, petiole, root and young leaves, including trichomes and stomata (Fig. 4-1a, b1, d1; Fig. 4-11b, c). These locations were substantially consistent with our previous report using heterologous promoter assays in Arabidopsis (summarized in Table 4-1). Therefore, it can be concluded that *CWPO-C* is expressed mainly in young tissues after differentiation, besides organs such as flowers and seeds, and is involved in the development or differentiation of organs and early growth. Interestingly, decapitation of poplar transformed with *Pcwpo-c*::*GUS* led to *CWPO-C* expression in the axillary meristems and in the newly generated branches. This result clearly shows that CWPO-C is involved during plant growth and development.

Several previous studies analyzed the functions of peroxidases by a reverse genetic approach in which targeted gene expression was suppressed or enhanced. In tobacco, tobacco transformants with suppressed anionic peroxidase (TOBPXDLF) showed an enhanced growth rate (Lagrimini et al. 1997). Overexpression of HRP, encoded by *prxC1a*, in hybrid

poplar resulted in higher growth rates (Kawaoka et al. 2003). These findings suggest that peroxidases have multiple roles during growth and development. In our current results, CWPO-C OE poplar lines (OE1, OE2, OE4) showed higher growth rates than the WT (Fig. 4-8b), yet there was no altered growth rate in CWPO-C RNAi suppression lines.

4-5. SUMMARY

In Chapter 2, CWPO-C was characterize by the use of model plant Arabidopsis and it was proposed that CWPO-C suppressed the growth of the plant. In this chapter, the transcription and localization of *CWPO-C* gene in poplar transgenics was analyzed. RT-qPCR analyzes indicated that *CWPO-C* was expressed in stem, leaves and roots meristematic tissues. Moreover, in the aerial part of the plant, *CWPO-C* expression was induced when the stem tip suffered decapitation, the outgrowth of axillary meristems showed strong *CWPO-C* expression, which indicates that CWPO-C might exert a substantive biological function in plant growth and development in Poplar. However, in comparison to Arabidopsis overexpressing CWPO-C, poplar OE lines showed enhanced growth of the stem in contrast to WT. Still, these findings suggest that peroxidases have a role during growth and development.

In the next Chapter, the focus turns to the lignification function of CWPO-C. So far, it was only demonstrated *in vitro* that CWPO-C was capable to oxidize monolignols and lignin polymer. Therefore, it is of interest to confirm with the use of overexpressing and suppressing

CWPO-C transgenics the lignin related function. The CWPO-C transgenics poplar were investigated by lignin content and composition analysis.

Chapter 5: *CWPO-C* expression affects gravitropism in Poplar and also alters lignin content and composition in Poplar

5-1. Introduction

In lignin biosynthesis, peroxidases use hydrogen peroxide in oxidizing monolignols (coniferyl and sinapyl alcohols in angiosperms), and the resulting radicals (G, guaiacyl and S, syringyl units) are polymerized into lignin (Boerjan et al. 2003). Lignin polymerization also requires the oxidization of the phenolic groups in lignin to continue the polymer growth (Sarkanen and Ludwig, 1971). So far, only CWPO-C peroxidase has been demonstrated to have oxidation activity towards large-size substrates such as S-oligo (polymerized oligomeric sinapyl alcohol) (Aoyama et al. 2002, Sasaki et al. 2004). The oxidation of substrates occurs at the amino acid residues, Tyr74 and Tyr177, avoiding steric hindrance of the substrates and proximity with the heme pocket (Sasaki et al. 2008, Shigeto et al. 2012). This oxidation capability makes CWPO-C a unique peroxidase, and because of its unique oxidizing abilities, CWPO-C has been believed to be a lignin polymerization-specific peroxidase.

5-2. Materials and Methods

5-2-1. Determination of acetyl bromide-soluble lignin (ABSL)

Stem samples were harvested from 6-week-old wild type plants and each transgenic line. They were ground to a powder in liquid nitrogen and then extracted with three washes of methanol. The extractive-free sample was freeze dried (CS-110 Scanvac, Lynge, Denmark) and used for further lignin analysis. The acetyl bromide lignin assay was performed as described by Barnes and Anderson (2017). The extractive-free, freeze-dried sample (ca. 5 mg) was digested with 1 mL of 25% acetyl bromide at 70°C for 1 h in a glass vial,

immediately cooled in ice, then 5 mL glacial acetic acid was added to complete the reaction. Later, 450 µL of the diluted sample was mixed with 1200 µL of 1.5 N NaOH and 900 µL of 0.5 M hydroxylamine hydrochloride, and the volume was adjusted to 3 mL with acetic acid. The absorbance at 280 nm of the mixture was recorded using a spectrophotometer (Shimadzu UV-1850, Japan). A blank sample was run as a control. The content percentage of lignin = $100 \cdot V \cdot (A_{sample} - A_{blank}) / Ɛ \cdot D \cdot L$ [where V = volume of the final solution (L); A = absorbance; Ɛ = molar extinction coefficient ($g^{-1} \cdot L \cdot cm^{-1}$); D = dry weight of the sample (g); L = cell thickness (cm)]. A molar extinction coefficient of 22.5 $g^{-1} \cdot L \cdot cm^{-1}$ was used for the calculation of percentage ABSL content.

5-2-2. Derivatization followed by reductive cleavage (DFRC)

The DFRC method was performed as described by Lu and Ralph (1997). Briefly, 10 mg of extractive-free sample in 3 mL acetyl bromide reagent (acetyl bromide/acetic acid, 20:80, v/v) was shaken at 90 rpm at 50°C for 3 h. The solvent was removed by rotary evaporation below 50°C. The evaporation residue was resuspended in 3 mL acidic reduction solvent (dioxane/acetic acid/water, 5:4:1, v/v/v). Following the addition of 50 mg zinc dust, the mixture was transferred into a separating funnel with 10 mL dichloromethane and saturated ammonium chloride. The internal standard, 0.1 mg of tetracosane, was added, and the aqueous phase was adjusted to between pH 2 and 3 using 3% HCl. After vigorous mixing, the organic layer was collected, and the extraction was repeated twice with 5 mL dichloromethane. The organic layer was dehydrated in magnesium sulfate, evaporated, , and acetylated overnight in 1.5 mL dichloromethane with 0.2 mL acetic anhydride and 0.2 mL pyridine. Once acetylation reagents were removed, the samples were dissolved in

dichloromethane and subjected to gas chromatography with a flame ionization detector (GC-FID). GC-FID analysis was performed using a Shimadzu GC-2014 (Shimadzu Co., Ltd., Kyoto, Japan) equipped with a InertCap-1 column (0.25 mm × 30 m; GL Sciences Inc., Tokyo, Japan). The temperature was programmed at a rate of 3°C min^{-1} from 140°C to 240°C and at 30°C min^{-1} from 240°C to 310°C. The final temperature (310°C) was held for 12 min. The amounts of coniferyl alcohol and sinapyl alcohol were determined using calibration curves derived from acetylated pure standards.

5-2-3. Histochemical assay and imaging

Cell walls were stained in stem sections of WT and transgenic plants using toluidine blue; lignins were detected using Wiesner staining. Plants were collected at 6 weeks old, and 20 μm cross-sections were cut from the first 0.5 cm of the basal parts of stems. Stems were embedded in Cryomatrix compound, then sections were prepared at −20°C. Cryomatrix was removed from the sections with water. Sections were then stained with 0.02% toluidine blue for 5 min (Pradhan Mitra and Loqué, 2014). Wiesner staining was performed as described by Euring et al. (2012), soaking sections in 1% (w/v) phloroglucinol for 3 min. Mounted sections were examined with a Keyence VHX-6000 optical microscope.

A time lapse camera TLC200 (Brinno, Taiwan) was used for gravitropic experiments. Poplar plants at 6 weeks old were positioned horizontally and imaged every minute for 24 h. The time the stem took to recover the 90° vertical position was recorded.

5-3. Results

5-3-1. Alteration of lignin content and composition

As shown in Fig. 4-1d1, d2, CWPO-C was expressed in xylem, and the protein has been shown to produce high molecular weight lignin *in vitro* (Aoyama et al. 2002). Also, knock-out of *CWPO-C* ortholog peroxidases, *AtPrx2*, *AtPrx25* and *AtPrx71* affected the lignin content and chemical structures in Arabidopsis (Shigeto et al. 2013). Therefore, we investigated whether overexpression or suppression of *CWPO-C* in poplar might affect lignin content and composition. Transgenic lines OE1 and RNAi1 at 6 weeks old were subjected to lignin analyses. Table 1 shows the lignin content determined by the acetyl bromide method and the arylglycerol-β-aryl (β-*O*-4) ether lignin composition, as determined by DFRC method. Lignin content in RNAi1 was significantly lower (45% decrease) than in the WT, while OE1 showed no difference from the WT (Table 5-1). A notable difference was found for the β-*O*-4 linkage in the lignin of RNAi1, in that the free guaiacyl monomer, coniferyl alcohol, was significantly higher than in WT (Table 5-1). Changes in lignin in RNAi1 were also observed using Wiesner staining of stem cross-sections. The fuchsia-color staining, related to lignified cell walls, seen in the stem cross-section was much reduced compared to the WT, and the distribution of lignified cells in the xylem was less uniform (Fig. 4-6b1–3). These chemical analyses and microscopic observations indicated that suppression of CWPO-C resulted in decreased lignin content and lower syringyl/guaiacyl (S/G) ratio in poplar.

5-3-2. Evaluation of relevance to auxin by gravitropism

Previously, we showed that overexpression of CWPO-C in Arabidopsis affected the phenotype strongly in way related to auxin (Yoshikay-Benitez et al. 2022). From the results in Chapter 4, it was clear that CWPO-C plays a role in organ development or differentiation during early growth of poplar, and it seemed possible that CWPO-C contributes to the catabolism of auxin. When a plant part is moved from a vertical to horizontal position, gravitropism occurs because of the altered distribution of auxin in the upper and lower part. In this study, we compared the time required to reach a 90° stem curvature after being placed horizontally. Transgenic OE1 plants bent more quickly than the WT, taking about half the time required by WT plants, at 8.2 h and 16.4 h, respectively (Fig. 5-1). Two other OE lines also showed shorter bending times than the WT. This result suggested the possibility that CWPO-C overexpression modulated the gravitropic response of the transgenic OE plants by affecting auxin accumulation. The difference in bending time between RNAi suppression lines and the WT was rather small fast, but still significant (Fig. 5-1).

Another notable phenotype related to auxin modification was found in the leaves: transgenic line OE1 showed more rounded leaf shape with less pronounced saw-tooth edges, while line RNAi1 had larger leaves with light green color, compared to the WT (Fig. 4-10). Because the hydathodes, at the leaf edge where notches develop, coincided with the expression site of CWPO-C (Fig. 4-11), we hypothesize that CWPO-C might function in an inhibitory manner on saw-tooth leaf formation in OE lines, resulting in the more rounded leaves.

Table 5-1 Lignin content and DFRC in WT and CWPO-C transgenic poplar

	Lignin (%)			µmol S/g lignin			µmol G/g lignin			S/G			µmol (S+G)/g lignin		
WT	9.2	±	0.8	61	±	20	428	±	40	0,14	±	0,03	489	±	60
RNAi1	5.1	±	0.6**	51	±	14	717	±	81**	0,07	±	0,01*	768	±	93**
OE1	8.8	±	0.9	45	±	14	381	±	74	0,12	±	0,03	426	±	84

Lignin content and monomer composition were measured by derivatization followed by reductive cleavage (DFRC). (*: $p < 0.05$, **: $p < 0.01$, Student's *t*-test).

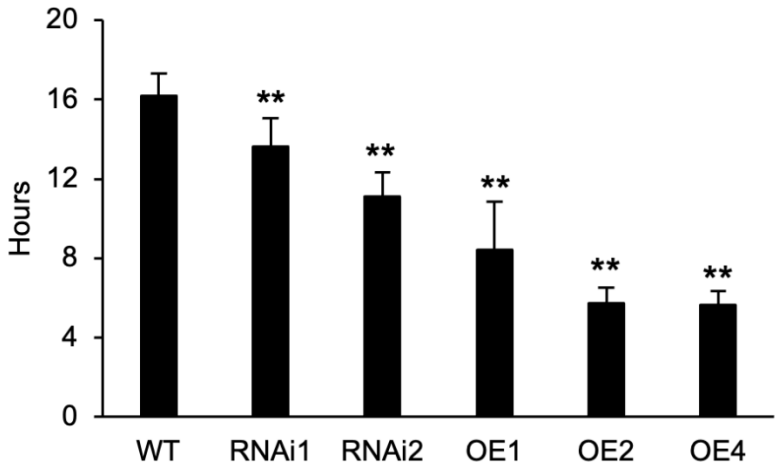

Fig. 5-1 Bending time of 6-week-old CWPO-C transgenics and WT poplar. Bending time refers to the time (h) required for the stem to return to standing at 90° from being placed horizontally. Mean ± standard deviation of four biological replicates. **: Significant difference ($p < 0.01$) compared with WT (Student's *t* test). OE1, OE2 and OE4: CWPO-C OE line 1, 2 and 4. RNAi1 and RNAi2: CWPO-C RNAi line 1 and 2

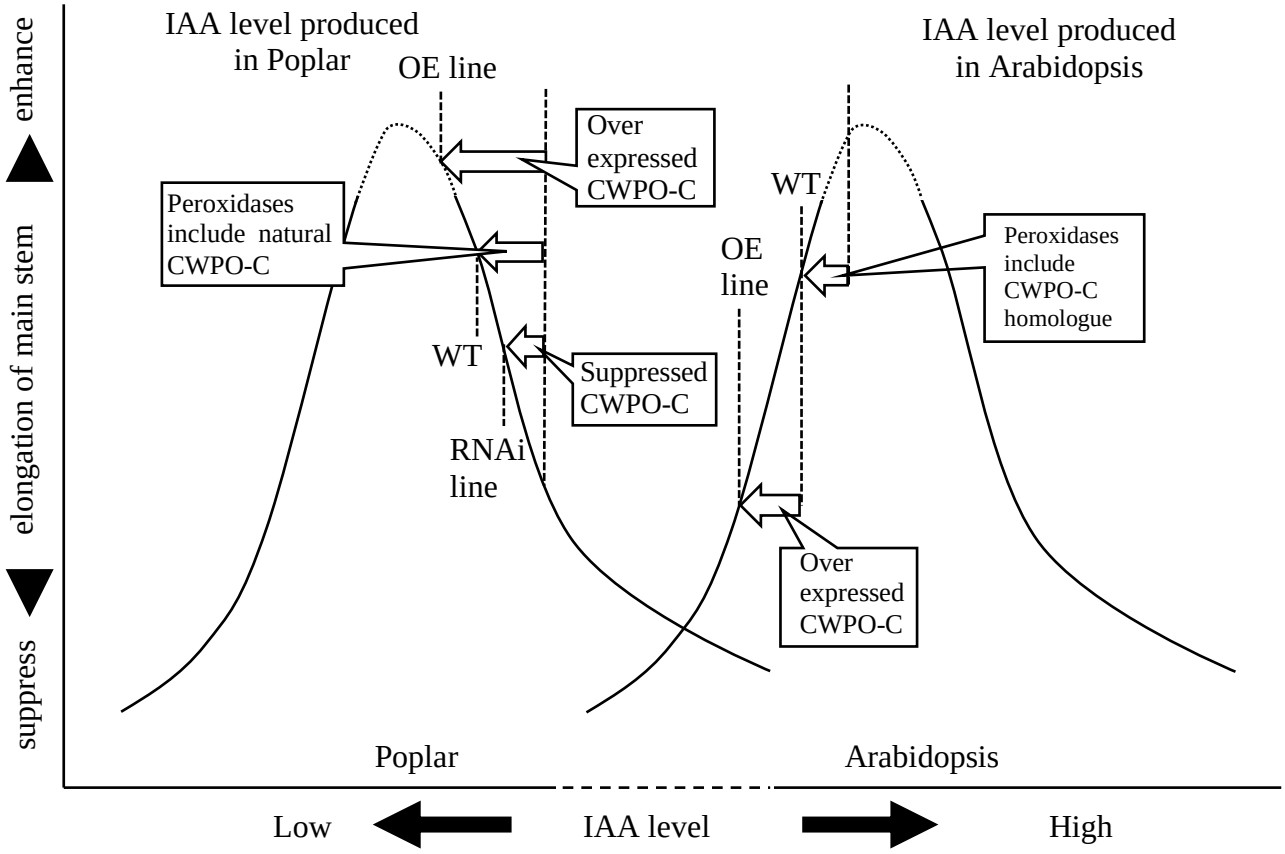

Fig. 5-2 Schematic representation of possible responses to altered *CWPO-C* expression in Arabidopsis and poplar. Stem elongation is promoted or inhibited over a range of auxin concentration, depending on the plant species and the effect of *CWPO-C* expression on auxin catabolism. In both poplar and Arabidopsis, overexpressed CWPO-C decreases IAA concentration via catabolism. In Arabidopsis, decreased IAA concentration leads to reduced elongation growth. In poplar, by contrast, overexpressed CWPO-C again decreases IAA concentration, but leads to enhanced elongation. The difference in apparent effects is presumed to result from different responses towards IAA concentration in the two plant species

5-4. Discussion

Interaction has been reported between auxin and peroxidase and can be divided broadly into two types: induction by auxin of peroxidases responsible for lignification, and auxin catabolism by peroxidases. For example, *AtPrx52*, which has been suggested to be involved in lignin biosynthesis, is regulated by auxin and other phytohormones (Herrero et al. 2014). The overexpression of *CpPrx01* from *Cucurbita pepo* in Arabidopsis led to longer roots and hypocotyls, at the same time reducing levels of the auxin indole-3-acetic acid (IAA) (Cosio et al. 2009). PxB2 from *Vitis vinifera* was found to have oxidative activity toward IAA, suggesting it played a role in controlling the amount of IAA in developing roots (Vatulescu et al. 2004). There have been no conclusive report on the cellular level localization where peroxidases interact with auxin in our knowledge. It is known that IAA is transported between cells through the apoplast, and IAA oxidase activity (catabolism) mainly occurs in the apoplast (Waldrum and Davies, 1981; García-Florenciano et al. 1992). Since CWPO-C was reported to be ionically-bound cell wall peroxidase (Tsutsumi et al. 1998), thus localized in the apoplast (Sasaki et al. 2006), we could predict that IAA catabolism by CWPO-C may occur in the apoplast. A gravitropism test is a traditional and simple method to observe alterations of auxin concentration. Here, the poplar CWPO-C OE lines, showed shorter recovery times for the stem to return to the vertical position (Fig. 5-1), which suggested that auxin amounts might be increased by the overexpression of *CWPO-C*. However, observations in Arabidopsis with overexpressing *CWPO-C* showed differences compared with the poplar OE lines (Yoshikay-Benitez et al. 2022): the CWPO-C OE Arabidopsis showed significantly longer recovery time (negative gravitropism) than the wild

type. The negative gravitropism was explained by a marked decrease of auxin content in CWPO-C OE Arabidopsis (Yoshikay-Benitez et al. 2022). Also, in Arabidopsis, CWPO-C OE caused severe suppression of stem elongation, whereas in poplar CWPO-C OE caused slightly enhanced stem elongation. One possible explanation for this apparent discrepancy is that poplar has a higher capability for maintenance of homeostasis against changes in auxin conditions. Another explanation is that such different phenotypes may be the result of different physiological responses between poplar and Arabidopsis, depending on the auxin concentration, as hypothesized in the schematic diagram (Fig. 5-2). In our previous study, the stem tip of Arabidopsis possessed approx. 2 ng/mg FW of IAA (Yoshikay-Benitez et al. 2022). Teichmann et al. (2008) showed that 4-month-old stem tips in poplar contained approx. 0.08 ng/mg FW of IAA. Sitbon et al. (1992) showed that tobacco shoot apex contained approx. 0.05 ng/mg FW of IAA. These reports suggested that the response and optimum concentrations of IAA are differed widely, depending on the plant species. It is also known that the reaction of plants to auxin differs, depending not only on the plant species, but also on the organ (Thimann 1969, Leopold 1955, Gaspar et al. 2003). In our previous report, recombinant CWPO-C protein broke down IAA *in vitro*, and IAA concentration in CWPO-C OE Arabidopsis was considerably reduced. Thus, we can conclude that overexpressed CWPO-C decreased endogenous IAA concentration. In our study, the observed effects of the CWPO-C OE on growth rate and bending time in poplar were directly opposite to those in Arabidopsis. A possible explanation for the different phenotypes is shown in Fig. 5-2, where the endogenous IAA concentration decreased towards the optimum in poplar, whereas it decreased away from the optimum in Arabidopsis. Concerning the bending time, the

mechanisms affecting bending time seems complicated. It seems difficult to explain relation of bending time and IAA concentration. The observed faster bending time of the CWPO-C OE poplar was opposite to CWPO-C OE Arabidopsis which showed the slower bending time. In addition, CWPO-C RNAi poplar showed a slightly faster or similar bending time than WT. In the case of poplar, it seems difficult to explain the changes of bending time by only IAA, and there are some other predominant factors for controlling the bending speed in poplar.

We considered the function of CWPO-C in lignification, because *CWPO-C* was expressed in the developing xylem during its progression to lignification, and *CWPO-C* suppression might affect the lignin content and S/G composition. Previously, three *CWPO-C* orthologs (*AtPrx2*, *AtPrx25*, and *AtPrx71*) were knocked out in Arabidopsis, and decreased lignin content was observed (Shigeto et al. 2013, 2015). Suppression of *NtPrx60* and *PrxA3a* genes in tobacco and aspen, respectively, also reduced the lignin content (Blee et al. 2003, Li et al. 2003). Knockout of orthologous genes (*AtPrx4*, *AtPrx52* and *AtPrx72*) of *Zinnia elegans* peroxidase, *ZePrx*, showed reduced lignin content and altered lignin composition (Fernández-Pérez et al. 2015a, 2015b; Herrero et al. 2013). In our current study, lignin content was reduced by 45% in the CWPO-C-suppressed poplar, and the S/G ratio of lignin in RNAi1 (determined by DFRC analysis) was half that of WT (Table 5-1). A noticeable increase in the content of the guaiacyl monomer, coniferyl alcohol, resulted in the decreased S/G ratio. The increase of guaiacyl monomer, after DFRC analysis, would be explained by an increase in β-*O*-4 linkage in guaiacyl lignin by the suppression of *CWPO-C*. It seems unlikely that suppression of a single peroxidase, an enzyme catalyzing the polymerization of monolignol, directly enhanced the biosynthesis of coniferyl alcohol. An alternative explanation might be that *CWPO-C*

suppression changed the allocation of S/G monolignol monomers at branch points in the biosynthetic pathway. The suppression of peroxidase activity might slow down the monolignol polymerization rate in the cell wall, so that the proportion of β-*O*-4 linkages increased in lignin through slower end-polymerization. This effect would be more prominent in guaiacyl lignin, because guaiacyl lignin was predominant in the young poplar plants used in this study. Previously, we observed a similar increase in the yield of DFRC products in knockout mutants of *AtPrx2*, *AtPrx25*, and *AtPrx71* (Shigeto et al. 2013, 2015). These results confirmed that CWPO-C and its Arabidopsis orthologs play a substantive role in lignin polymerization in the cell wall.

5-5. SUMMARY

This Chapter proved that CWPO-C was capable to alter the lignin content and composition *in vivo*. CWPO-C was responsible for the lignin content and S/G ratio alterations. The result of the lignin content in RNAi1 was significantly lower, by 45% decrease, than in the WT and OE1. Moreover, the syringyl/guaiacyl (S/G) ratio was also decreased in RNAi1. These analyzes and microscopic observations clearly indicated that suppression of *CWPO-C* had a strong effect over the lignin polymer in Poplar.

In Chapter 4, the expression and phenotypic analysis using transgenic and wild type Poplar, in addition to the gravitropism results showed in this Chapter, do not contradict the assumption that CWPO-C could affect auxin concentration and plays a role in early plant growth or differentiation in poplar. Comprehension of the amount of auxin and auxin

metabolites in wild type and transgenic plants with different expression level of *CWPO-C*, as well as determining the role of CWPO-C at the molecular level in poplar results of great interest in next studies.

Chapter 6: FINAL REMARKS

FINAL REMARKS

In this study, it was found that *CWPO-C* was expressed in the xylem, shoot, young flowers, developing xylem and leaf. These results suggests that the CWPO-C peroxidase is expressed in not only in aim to lignification tissues but also is involved in meristematic and plant development tissues. Moreover, CWPO-C-OE, displayed shorter stems compared with the WT plants in Arabidopsis. Interestingly, some CWPO-C-OE plants exhibited a peculiar phenotypic feature during the early stages of bolting, CWPO-C-OE plants showed a curled apical stem tip. The presence of curled apical tip phenotype negatively affected plant growth, leading to dwarfism in Arabidopsis. Generally, curled apical tip is known to be a phenotype characteristic of plants with auxin alterations. Auxin accumulation in plants was evaluated by gravitropism assay and CWPO-C-OE plants showed slower bending time than WT, sign of decreased IAA amount. These observations on plant growth and stem gravitropism suggested that CWPO-C affects auxin concentration. Suggesting a new role for the CWPO-C peroxidase.

IAA was quantified in WT and transgenic CWPO-C-OE stem. Both CWPO-C-OE phenotypes, straight and curled apical tips showed lower IAA content in contrast to WT. This result strongly suggested that CWPO-C plays a role in the regulation of plant growth through the catabolizing IAA.

In poplar, Real time PCR analysis and observed promoter expression of *CWPO-C*, revealed that CWPO-C was strongly expressed in immature tissues such as the upper stem, axillary buds and young leaves. These organs, expression and localization in poplar, were comparable

to the organs characterization in the Arabidopsis *CWPO-C* promoter plants. However, in poplar CWPO-C-OE line, the stem growth was enhanced, as well as, the gravitropic bending time was accelerated in comparison to WT. In the contrary of Arabidopsis CWPO-C-OE, where it was observed stem dwarfism and delayed gravitropic bending time. It is hypothesized that a homeostasis response is activated in poplar or depending on the auxin concentration, physiological responses vary between Arabidopsis and poplar. Yet, these results suggest that CWPO-C is involved in vertical growth and gravitropic response.

Concerning the previous *in vitro* assay, which showed CWPO-C to be capable of lignification, in addition to the GUS assay and Real time PCR analysis that also revealed *CWPO-C* expression in developing xylem of the stem, for both, Arabidopsis and poplar; histochemical assays revealed that in CWPO-C absence plant, xylem tissue decreased area in comparison to WT. Thus, the lignin content in CWPO-C absence plant was significantly lower and the syringyl/guaiacyl (S/G) ratio was also decreased. Explanation for the lignification alteration could be the natural increase of guaiacyl monomer concentration in young poplar plants, or the slower monolignol polymerization rate in the cell wall in the absence of the peroxidase CWPO-C. These chemical analyzes demonstrated that CWPO-C plays a substantive role in the lignin polymerization of the cell wall *in vivo*, confirming previous *in vitro* evidence.

Our results demonstrated that CWPO-C plays a role in differentiation and plant early growth, as well as in lignin polymerization. Thus, results in this study set up a new catabolic pathway for auxin in addition to the known auxin regulating system.

REFERENCES

Abbott E, Hall D, Hamberger B, Bohlmann J (2010) Laser microdissection of conifer stem tissues: Isolation and analysis of high quality RNA, terpene synthase enzyme activity and terpenoid metabolites from resin ducts and cambial zone tissue of white spruce (*Picea glauca*). *BMC Plant Biology,* 10, 106. https://doi.org/10.1186/1471-2229-10-106

Adler, E (1977). Lignin chemistry—past, present and future. *Wood science and technology*, 11(3), 169-218. https://doi.org/10.1007/BF00365615

Almagro L, Gómez Ros LV, Belchi-Navarro S, Bru R, Ros Barceló A, Pedreño MA (2009) Class III peroxidases in plant defense reactions. *Journal of Experimental Botany*, 60(2):377-90. https://doi.org/10.1093/jxb/ern277

Aloni R (2001) Foliar and Axial Aspects of Vascular Differentiation: Hypotheses and Evidence. *Journal of Plant Growth Regulation*, 20(1). https://doi.org/10.1007/s003440010001

Aloni R, Schwalm K, Langhans M, Ullrich CI (2003) Gradual shifts in sites of free-auxin production during leaf-primordium development and their role in vascular differentiation and leaf morphogenesis in Arabidopsis. *Planta,* 216, 841–853. https://doi.org/10.1007/s00425-002-0937-8

Aoyama W, Sasaki S, Matsumura S, Hirai H, Tsutsumi Y, Nishida T (2002) Sinapyl alcohol-specifc peroxidase isoenzyme catalyzes the formation of the dehydrogenative polymer

from sinapyl alcohol. *Journal of Wood Science,* 48:497–504. https://doi.org/10.1007/BF00766646

Araiso T, Miyoshi K, Yamazaki I (1976) Mechanisms of electron transfer from sulfite to horseradish peroxidase-hydroperoxide compounds. *Biochemistry*, 15(14), 3059-3063.

Bandurski RS, Schulze A, Dayanandan P, Kaufman PB (1984) Response to Gravity by *Zea mays* Seedlings: I. Time Course of the Response. *Plant physiology*, 74(2), 284-288. https://doi.org/10.1104/pp.74.2.284

Barceló AR, Pomar F (2001) Oxidation of cinnamyl alcohols and aldehydes by a basic peroxidase from lignifying *Zinnia elegans* hypocotyls. *Phytochemistry*, 57(7), 1105-1113. https://doi.org/10.1016/S0031-9422(01)00050-4

Barnes WJ, Anderson CT (2017) Acetyl Bromide Soluble Lignin (ABSL) Assay for Total Lignin Quantification from Plant Biomass. *Bio-Protocol Journal*, 7(5):e2149. https://doi.org/10.21769/BioProtoc.2149

Blancaflor EB, Masson PH (2003) Plant gravitropism. Unraveling the ups and downs of a complex process. *Plant physiology*, 133(4), 1677-1690. https://doi.org/10.1104/pp.103.032169

Blee KA, Choi JW, O'Connell AP, Schuch W, Lewis NG, & Bolwell GP (2003) A lignin-specific peroxidase in tobacco whose antisense suppression leads to vascular tissue modification. *Phytochemistry*, 64(1), 163-176. https://doi.org/10.1016/S0031-9422(03)00212-7

Boerjan W, Ralph J, Baucher M (2003) Lignin biosynthesis. *Annual Review of Plant Biology*, 54:519-46. https://doi.org/10.1146/annurev.arplant.54.031902.134938

Bredmose N, Costes E (2003) Axillary Bud Growth. Growth Regulation. *Encyclopedia of Rose Science*, Pages 374-381. https://doi.org/10.1016/B978-0-12-809633-8.05056-1

Campbell MM, Sederoff RR (1996) Variation in Lignin Content and Composition (Mechanisms of Control and Implications for the Genetic Improvement of Plants). *Plant Physiology*, 110(1):3-13. https://doi.org/10.1104/pp.110.1.3.

Chen Q, Dai X, De-Paoli H, Cheng Y, Takebayashi Y, Kasahara H, Kamiya Y, Zhao Y (2014) Auxin overproduction in shoots cannot rescue auxin deficiencies in Arabidopsis roots. *Plant Cell Physiology*, 55(6):1072–1079. https://doi.org/10.1093/pcp/pcu039

Cheng Y, Dai X, Zhao Y (2006) Auxin biosynthesis by the YUCCA favin monooxygenases controls the formation of floral organs and vascular tissues in Arabidopsis. *Genes and Development*, 20(13):1790–1799. https://doi.org/10.1101/gad.1415106

Clough SJ, Bent AF (1998) Floral dip: a simplifed method for Agrobacterium-mediated transformation of *Arabidopsis thaliana*. *Plant Journal*, 16:735–743. https://doi.org/10.1046/j.1365-313x.1998.00343.x

Cosio C, Vuillemin L, De Meyer M, Kevers C, Penel C, Dunand C (2009) An anionic class III peroxidase from zucchini may regulate hypocotyl elongation through its auxin oxidase activity. *Planta*, 229(4):823–836. https://doi.org/10.1007/s00425-008-0876-0

Davies PJ (1995) The plant hormone concept: concentration, sensitivity and transport. In: Davies PJ (ed) *Plant hormones*, pp 13–38. https://doi.org/10.1007/978-94-011-0473-9_2

Davies PJ (2010) The plant hormones: their nature, occurrence, and functions. In *Plant hormones* (pp. 1-15). Springer, Dordrecht. https://doi.org/10.1007/978-1-4020-2686-7_1

Dolphin D, Forman A, Borg DC, Fajer J, Felton RH (1971) Compounds I of catalase and horse radish peroxidase: π-cation radicals. *Proceedings of the National Academy of Sciences*, 68(3), 614-618. https://doi.org/10.1073/pnas.68.3.614

Donaldson LA (1991) Seasonal changes in lignin distribution during tracheid development in *Pinus radiata* D. Don. *Wood Science and Technology*, 25(1), 15-24. https://doi.org/10.1007/BF00195553

Doyle WA, Blodig W, Veitch NC, Piontek K, Smith AT (1998) Two substrate interaction sites in lignin peroxidase revealed by site directed mutagenesis. *Biochemistry,* 37:15 097–15105. https://doi.org/10.1021/bi981633h

Euring D, Löfke C, Teichmann T, Polle A (2012) Nitrogen fertilization has diferential efects on N allocation and lignin in two *Populus* species with contrasting ecology. *Trees,* 26:1933–1942. https://doi.org/10.1007/s00468-012-0761-0

Fernández-Pérez F, Vivar T, Pomar F, Pedreño MA, Novo-Uzal E (2015a) Peroxidase 4 is involved in syringyl lignin formation in *Arabidopsis thaliana*. *Journal of Plant Physiology,* 175, 86-94. https://doi.org/10.1016/j.jplph.2014.11.006

Fernández-Pérez F, Pomar F, Pedreño MA, Novo-Uzal E (2015b) The suppression of AtPrx52 affects fibers but not xylem lignification in Arabidopsis by altering the proportion of syringyl units. *Physiology Plantarum*, 154: 395-406. https://doi.org/10.1111/ppl.12310

Freudenberg K, Neish AC (1968) *Constitution and Biosynthesis of Lignin*. Springer-Verlag, Berlin, 129. http://dx.doi.org/10.1007/978-3-642-85981-6

Gabaldón C, López-Serrano M, Pedreño MA, Barceló AR (2005) Cloning and molecular characterization of the basic peroxidase isoenzyme from *Zinnia elegans*, an enzyme involved in lignin biosynthesis. *Plant physiology*, 139(3), 1138-1154. https://doi.org/10.1104/pp.105.069674

Galston WA, Bonner J, Baker SR (1953) Flavoprotein and peroxidase as components of the indolacetic acid oxidase system of peas. *Archives Biochemistry and Biophysics*, Vol 42:456–470. https://doi.org/10.1016/0003-9861(53)90373-7

García-Florenciano E, Calderón AA, R. Muñoz R, Ros Barceló A (1992) The Decarboxylative Pathway of lndole-3-Acetic Acid Catabolism is not Functional in Grapevine Protoplasts. *Journal of Experimental Botany*, Volume 43, Issue 5, Pages 715–721. https://doi.org/10.1093/jxb/43.5.715

Gaspar T, Kevers C, Hausman JF, Ripetti V (1994) Peroxidase activity and endogenous free auxin during adventitious root formation. In: Lumsden, P.J., Nicholas, J.R., Davies, W.J. (eds) *Physiology, Growth and Development of Plants in Culture*. Springer, Dordrecht. https://doi.org/10.1007/978-94-011-0790-7_32

Gaspar T, Kevers C, Faivre-Rampant O, Crèvecoeur M, Penel CL, Greppin H, Dommes J (2003) Changing concepts in plant hormone action. *In Vitro Cellular and Developmental Biology-Plant*, 39, 85–106. https://doi.org/10.1079/IVP2002393

Gazaryan IG, Lagrimini LM, Ashby GA, Thorneley RN (1996) Mechanism of indole-3-acetic acid oxidation by plant peroxidases: anaerobic stopped-flow spectrophotometric studies on horseradish and tobacco peroxidases. *Biochemical Journal*, https://doi.org/10.1042/bj3130841.

Goring DAI, Saka S, Higuchi T (1988) Localization of lignins in wood cell walls. *Biosynthesis and biodegradation of wood components*, 51-62. Academic Press Inc.

Gutjahr C, Riemann M, Müller A (2005) Cholodny–went revisited: a role for jasmonate in gravitropism of rice coleoptiles. *Planta,* 222:575–585. https://doi.org/10.1007/s00425-005-0001-6

Harris RZ, Newmyer SL, De Montellano PO (1993) Horseradish peroxidase-catalyzed two-electron oxidations. Oxidation of iodide, thioanisoles, and phenols at distinct sites. *Journal of Biological Chemistry*, 268(3), 1637-1645. https://doi.org/10.1016/S0021-9258(18)53900-4

Herrero J, Fernández-Pérez F, Yebra T, Novo-Uzal E, Pomar F, Pedreño MA, Cuello J, Guéra A, Esteban-Carrasco A, Zapata JM (2013) Bioinformatic and functional characterization of the basic peroxidase 72 from *Arabidopsis thaliana* involved in lignin biosynthesis. *Planta*, 237, 1599–1612. https://doi.org/10.1007/s00425-013-1865-5

Herrero J, Esteban-Carrasco A, Zapata JM (2014) *Arabidopsis thaliana* peroxidases involved in lignin biosynthesis: *In silico* promoter analysis and hormonal regulation. *Plant Physiology and Biochemistry*, 80:192-202. https://doi.org/10.1016/j.plaphy.2014.03.027

Hinman RL, Lang J (1965) Peroxidase-catalyzed oxidation of indole3-acetic acid. *Biochemistry*, 4(1):144–158. https://doi.org/10.1021/bi00877a023

Hoffmann N, Benske A, Betz H, Schuetz M, Samuels AL (2020) Laccases and Peroxidases Co-Localize in Lignified Secondary Cell Walls throughout Stem Development. *Plant Physiology*, 184(2):806-822. https://doi.org/10.1104/pp.20.00473

Hoson T (1993) Regulation of polysaccharide breakdown during auxin-induced cell wall loosening. *Journal of Plant Research*, 106: 369–381. https://doi.org/10.1007/BF02345982

Humphreys JM, Chapple C (2002). Rewriting the lignin roadmap. *Current opinion in plant biology*, 5(3), 224-229. https://doi.org/10.1016/S1369-5266(02)00257-1

Jefferson RA, Kavanagh TA, Bevan MW (1987) GUS fusions: betaglucuronidase as a sensitive and versatile gene fusion marker in higher plants. *EMBO Journal*, 6:3901–3907. https://doi.org/10.1002/j.1460-2075.1987.tb02730.x

Jemmat AM, Ranocha P, Le Ru A, Neel M, Jauneau A, Raggi S, Ferrari S, Burlat V, Dunand C (2020) Coordination of five class III peroxidase-encoding genes for early germination events of *Arabidopsis thaliana*. *Plant Science*, https://doi.org/10.1016/j.plantsci.2020.110565

Jin J, Hewezi T, Baum TJ (2011) Arabidopsis peroxidase AtPRX53 influences cell elongation and susceptibility to *Heterodera schachtii*. *Plant signaling & behavior*, 6(11), 1778-1786. https://doi.org/10.4161/psb.6.11.17684

Kawaoka A, Kawamoto T, Moriki H, Murakami A, Murakami K, Yoshida K, Sekine M, Takano M, Shinmyo A (1994) Growth-stimulation of tobacco plant introduced the horseradish peroxidase gene prxC1a. *Journal of fermentation and bioengineering*, 78(1), 49-53. https://doi.org/10.1016/0922-338X(94)90177-5

Kawaoka A, Matsunaga E, Endo S, Kondo S, Yoshida K, Shinmyo A, Ebinuma H (2003) Ectopic Expression of a Horseradish Peroxidase Enhances Growth Rate and Increases Oxidative Stress Resistance in Hybrid Aspen. *Plant Physiology*, 132(3), 1177-1185. https://doi.org/10.1104/pp.102.019794

Kijidani Y, Ohshiro N, Iwata D, Nagamine M, Nishiyama T, Matsumura J, Koga S (2014) Variation of indole acetic acid (IAA) amounts in cambial-region tissues in 7- and 24-year-old sugi (*Cryptomeria japonica*) trees. *Journal of Wood Science*, 60:177–185. https://doi.org/10.1007/s10086-014-1394-2

Kobayashi S, Nakano M, Kimura T, Schaap AP (1987) On the mechanism of the peroxidase-catalyzed oxygen-transfer reaction. *Biochemistry*, 26(16), 5019-5022.

Kowalczyk M, Sandberg G (2001) Quantitative Analysis of Indole-3-Acetic Acid Metabolites in Arabidopsis, *Plant Physiology*, Volume 127, Issue 4, Pages 1845–1853. https://doi.org/10.1104/pp.010525

Kunieda T, Shimada T, Kondo M, Nishimura M, Nishitani K, Hara Nishimura I (2013) Spatiotemporal secretion of PEROXIDASE36 is required for seed coat mucilage extrusion in Arabidopsis. *Plant Cell*, 25:1355–1367. https://doi.org/10.1105/tpc.113.110072

Lagrimini LM, Gingas V, Finger F, Rothstein S, Liu T (1997) Characterization of Antisense Transformed Plants Deficient in the Tobacco Anionic Peroxidase. *Plant Physiology*, 114(4):1187-1196. https://doi.org/10.1104/pp.114.4.1187

Leopold AC (1955) Auxins and Plant Growth. University of California Press, Berkeley and Los Angeles.

Li L, Popko JL, Umezawa T, Chiang VL (2000) 5-Hydroxyconiferyl aldehyde modulates enzymatic methylation for syringyl monolignol formation, a new view of monolignol biosynthesis in angiosperms. *Journal of Biological Chemistry*, 275(9), 6537-6545. https://doi.org/10.1074/jbc.275.9.6537

Li L, Cheng XF, Leshkevich J, Umezawa T, Harding SA, Chiang VL (2001) The last step of syringyl monolignol biosynthesis in angiosperms is regulated by a novel gene encoding sinapyl alcohol dehydrogenase. *The Plant Cell*, 13(7), 1567-1586. https://doi.org/10.1105/TPC.010111

Li Y, Kajita S, Kawai S, Katayama Y, Morohoshi N (2003) Down-regulation of an anionic peroxidase in transgenic aspen and its effect on lignin characteristics. *Journal of Plant Research*, 116, 175–182. https://doi.org/10.1007/s10265-003-0087-5

Liszkay A, Kenk B, Schopfer P (2003) Evidence for the involvement of cell wall peroxidase in the generation of hydroxyl radicals mediating extension growth. *Planta*, 217:658–667. https://doi.org/10.1007/s00425-003-1028-1

Liszkay A, van der Zalm E, Schopfer P (2004) Production of reactive oxygen intermediates (O2−, H2O2, and OH) by maize roots and their role in wall loosening and elongation growth. *Plant physiology*, 136(2), 3114-3123. https://doi.org/10.1104/pp.104.044784

Lu F, Ralph J (1997) Derivatization followed by reductive cleavage (DFRC method), a new method for lignin analysis: protocol for analysis of DFRC monomers. *Journal of Agricultural and Food Chemistry*, 45(7), 2590-2592. https://doi.org/10.1021/jf970258h

Ludwig-Müller J (2011) Auxin conjugates: their role for plant development and in the evolution of land plants. *Journal of Experimental Botany*, 62 (6): 1757–1773. https://doi.org/10.1093/jxb/erq412

Marjamaa K, Hildén K, Kukkola E, Lehtonen M, Holkeri H, Haapaniemi P, Koutaniemi S, Teeri TH, Fagerstedt K, Lundell T (2006) Cloning, characterization and localization of three novel class III peroxidases in lignifying xylem of Norway spruce (*Picea abies*). *Plant molecular biology*, 61(4), 719-732. https://doi.org/10.1007/s11103-006-0043-6

Mäder M, Nessel A, Bopp M (1977) Über die physiologische Bedeutung der Peroxidase-Isoenzymgruppen des Tabaks anhand einiger biochemischer Eigenschaften: II. pH-Optima, Michaelis-Konstanten, Maximale Oxidationsraten. *Zeitschrift für Pflanzenphysiologie*, 82(3), 247-260. https://doi.org/10.1016/S0044-328X(77)80059-7

Miki Y, Calviño FR, Pogni R, Giansanti S, Ruiz-Dueñas FJ, Martínez MJ, Basosi R, Romero A, Martínez AT (2011) Crystallographic, kinetic, and spectroscopic study of the first ligninolytic peroxidase presenting a catalytic tyrosine. *Journal of Biological Chemistry*, 286:15525–15534. https://doi.org/10.1074/jbc.M111.220996

Moss TH, Ehrenberg A, Bearden AJ (1969) Mössbauer spectroscopic evidence for the electronic configuration of iron in horseradish peroxidase and its peroxide derivatives. *Biochemistry*, 8(10), 4159-4162.

Muday GK (2001) Auxins and tropisms. *Journal of plant growth regulation*, 20(3).

Muday GK, Murphy AS (2002) An emerging model of auxin transport regulation. *The Plant Cell*, 14(2), 293-299. https://doi.org/10.1105/tpc.140230

Müller K, Linkies A, Vreeburg RA, Fry SC, Krieger-Liszkay A, Leubner-Metzger G (2009) *In vivo* cell wall loosening by hydroxyl radicals during cress seed germination and elongation growth. *Plant Physiology*, 150: 1855–1865. https://doi.org/10.1104/pp.109.139204

Nanasato Y, Kido M, Kato A, Ueda T, Suharsono S, Widyastuti U, Tsujimoto H, Akashi K (2015) Efficient genetic transformation of *Jatropha curcas* L. by means of vacuum infiltration combined with filter-paper wicks. *In Vitro Cellular and. Devevelopmental. Biology-Plant* 51, 399–406. https://doi.org/10.1007/s11627-015-9703-z

Nishiguchi M, Yoshida K, Mohri T, Igasaki T, Shinohara K (2006) An improved transformation system for Lombardy poplar (*Populus nigra* var. *italica*). *Journal of Forestry Research*, 11:175–180. https://doi.org/10.1007/s10310-006-0203-1

Olson PD, Varner JE (1993) Hydrogen peroxide and lignification. *The Plant Journal*, 4(5), 887-892. https://doi.org/10.1046/j.1365-313X.1993.04050887.x

Osakabe K, Koyama H, Kawai S, Katayama Y, Morohoshi N (1995) Molecular cloning of two tandemly arranged peroxidase genes from *Populus kitakamiensis* and their differential regulation in the stem. *Plant molecular biology*, 28(4), 677-689. https://doi.org/10.1007/BF00021193

Osakabe K, Tsao CC, Li L, Popko JL, Umezawa T, Carraway DT, Smeltzer RH, Joshi CP, Chiang VL (1999) Coniferyl aldehyde 5-hydroxylation and methylation direct syringyl lignin biosynthesis in angiosperms. *Proceedings of the National Academy of Sciences*, 96(16), 8955-8960. https://doi.org/10.1073/pnas.96.16.8955

Østergaard L, Teilum K, Mirza O, Mattsson O, Petersen M, Welinder KG, Mundy J, Gajhede M, Henriksen A (2000) Arabidopsis ATP A2 peroxidase. Expression and high-resolution structure of a plant peroxidase with implications for lignification. *Plant Molecular Biology*, 44(2), 231-243. https://doi.org/10.1023/A:1006442618860

Parvathi K, Chen F, Guo D, Blount JW, Dixon RA (2001) Substrate preferences of O-methyltransferases in alfalfa suggest new pathways for 3-O-methylation of monolignols. *The Plant Journal*, 25: 193-202. https://doi.org/10.1111/j.1365-313X.2001.00956.x

Pickard BG (1985) Roles of Hormones in Phototropism. In: Pharis, R.P., Reid, D.M. (eds) Hormonal Regulation of Development III. *Encyclopedia of Plant Physiology*, vol 11. Springer, Berlin, Heidelberg. https://doi.org/10.1007/978-3-642-67734-2_11

Pradhan Mitra P, Loqué D (2014) Histochemical staining of *Arabidopsis thaliana* secondary cell wall elements. *Journal of Visualized Experiments,* (87):51381. https://doi.org/10.3791/51381

Ruiz-Dueñas FJ, Morales M, Garcia E, Miki Y, Martínez MJ, Martínez AT (2009) Substrate oxidation sites in versatile peroxidase and other basidiomycete peroxidases. *Journal of Experimental Botany,* 60:441–452. https://doi.org/10.1093/jxb/ern261

Rakusová H, Gallego-Bartolomé J, Vanstraelen M, Robert HS, Alabadí D, Blázquez MA, Benková E, Friml J (2011) Polarization of PIN3-dependent auxin transport for hypocotyl gravitropic response in *Arabidopsis thaliana*. *The Plant Journal,* 67:817–826. https://doi.org/10.1111/j.1365-313X.2011.04636.x

Ren LL, Liu YJ, Liu HJ, Qian TT, Qi LW, Wang XR, Zeng QY (2014) Subcellular relocalization and positive selection play key roles in the retention of duplicate genes of Populus class III peroxidase family. *Plant Cell,* 26: 2404–2419. https://doi.org/10.1105/tpc.114.124750

Renard, J, Martínez-Almonacid, I, Sonntag, A, Molina I, Moya-Cuevas J, Bissoli G, Muñoz-Bertomeu J, Faus I, Niñoles R, Shigeto J, Tsutsumi Y, Gadea J, Serrano R, Bueso E (2020) PRX2 and PRX25, peroxidases regulated by COG1, are involved in seed longevity in Arabidopsis. *Plant Cell Environment,* 43: 315– 326. https://doi.org/10.1111/pce.13656

Salisbury FB, Gillespie L, Rorabaugh P (1988) Gravitropism in higher plant shoots. *Plant Physiology*, 88:1186–1194. https://doi.org/10.1104/pp.88.4.1186

Samuels A, Rensing K, Douglas C, Mansfield S, Dharmawardhana D, & Ellis B (2002). Cellular machinery of wood production: differentiation of secondary xylem in *Pinus contorta* var. latifolia. *Planta*, 216, 72-82. https://doi.org/10.1007/s00425-002-0884-4

Santiago R, Barros-Rios J, Malvar RA (2013) Impact of Cell Wall Composition on Maize Resistance to Pests and Diseases. *International Journal of Molecular Sciences*, 14(4):6960-6980. https://doi.org/10.3390/ijms14046960

Sarkanen KV, Ludwig CH (1971) Lignins, Occurrence, Formation, Structure and Reactions. John Wiley & Sons, Inc., New York.

Sasaki S, Nishida T, Tsutsumi Y, Kondo R (2004) Lignin dehydrogenative polymerization mechanism: a poplar cell wall peroxidase directly oxidizes polymer lignin and produces *in vitro* dehydrogenative polymer rich in beta-*O*-4 linkage. *FEBS Letters*, 562:197–201. https://doi.org/10.1016/S0014-5793(04)00224-8

Sasaki S, Baba K, Nishida T, Tsutsumi Y, Kondo R (2006) The cationic cell-wall-peroxidase having oxidation ability for polymeric substrate participates in the late stage of lignification of *Populus alba* L. *Plant Molecular Biology*, 62:797–807. https://doi.org/10.1007/s11103-006-9057-3

Sasaki S, Nonaka D, Wariishi H, Tsutsumi Y, Kondo R (2008) Role of Tyr residues on the protein surface of cationic cell-wall-peroxidase (CWPO-C) from poplar: potential

oxidation sites for oxidative polymerization of lignin. *Phytochemistry,* 69:348–355. https://doi.org/10.1016/j.phytochem.2007.08.020

Schmid J, & Amrhein N (1995) Molecular organization of the shikimate pathway in higher plants. *Phytochemistry*, 39(4), 737-749. https://doi.org/10.1016/0031-9422(94)00962-S

Schwark A, Schierle J (1992) Interaction of ethylene and auxin in the regulation of hook growth I the role of auxin in different growing regions of the hypocotyl hook of *Phaseolus vulgaris*. *Journal of Plant Physiology*, 140(5), 562-570. https://doi.org/10.1016/S0176-1617(11)80790-X

Shigeto J, Itoh Y, Tsutsumi Y, Kondo R (2012) Identification of Tyr74 and Tyr177 as substrate oxidation sites in cationic cell wall-bound peroxidase from *Populus alba* L. *FEBS Journal,* 279:348–357. https://doi.org/10.1111/j.1742-4658.2011.08429.x

Shigeto J, Kiyonaga Y, Fujita K, Kondo R, Tsutsumi Y (2013) Putative cationic cell-wall-bound peroxidase homologues in Arabidopsis, AtPrx2, AtPrx25, and AtPrx71, are involved in lignification. *Journal of Agricultural and Food Chemistry,* 61:3781–3788. https://doi.org/10.1021/jf400426g

Shigeto J, Nagano M, Fujita K, Tsutsumi Y (2014) Catalytic profile of Arabidopsis peroxidases, AtPrx-2, 25 and 71, contributing to stem lignification. *PLoS ONE,* 9(8):e105332. https://doi.org/10.1371/journal.pone.0105332

Shigeto J, Itoh Y, Hirao S, Ohira K, Fujita K, Tsutsumi Y (2015) Simultaneously disrupting AtPrx2, AtPrx25 and AtPrx71 alters lignin content and structure in Arabidopsis stem. *Journal of Integrative Plant Biology*, 57:349–356. https://doi.org/10.1111/jipb.12334

Shigeto J and Tsutsumi Y (2016) Diverse functions and reactions of class III peroxidases. *New Phytologist*, 209: 1395-1402. https://doi.org/10.1111/nph.13738

Sieburth LE (1999) Auxin is required for leaf vein pattern in Arabidopsis. *Plant Physiology*, 121(4), 1179-1190. https://doi.org/10.1104/pp.121.4.1179

Sitbon F, Hennion S, Sundberg B, Little CH, Olsson O, Sandberg G (1992) Transgenic Tobacco Plants Coexpressing the *Agrobacterium tumefaciens* iaaM and iaaH Genes Display Altered Growth and Indoleacetic Acid Metabolism. *Plant Physiology*, 99(3):1062-9. https://doi.org/10.1104/pp.99.3.1062

Sitter AJ, Reczek CM, Terner J (1985) Heme-linked ionization of horseradish peroxidase compound II monitored by the resonance Raman Fe (IV)= O stretching vibration. *Journal of Biological Chemistry*, 260(12), 7515-7522. https://doi.org/10.1016/S0021-9258(17)39637-0

Song C, Lu L, Guo Y, Xu H, Li R (2019) Efficient Agrobacterium-Mediated Transformation of the Commercial Hybrid Poplar *Populus Alba* × *Populus glandulosa* Uyeki. *International Journal of Molecular Sciences,* 20, 2594. https://doi.org/10.3390/ijms20102594

Steeves V, Förster H, Pommer U, Savidge R (2001) Coniferyl alcohol metabolism in conifers—I. Glucosidic turnover of cinnamyl aldehydes by UDPG: coniferyl alcohol glucosyltransferase from pine cambium. *Phytochemistry*, 57(7), 1085-1093. https://doi.org/10.1016/S0031-9422(01)00107-8

Takata N, Eriksson ME (2012) A simple and efficient transient transformation for hybrid aspen (*Populus tremula* × *P. tremuloides*). *Plant Methods*, 8, 30. https://doi.org/10.1186/1746-4811-8-30

Takeuchi M, Watanabe A, Tamura M, Tsutsumi Y (2018) The gene expression analysis of Arabidopsis thaliana ABC transporters by real-time PCR for screening monolignol-transporter candidates. *Journal of Wood Science*, 64, 477–484. https://doi.org/10.1007/s10086-018-1733-9

Tanaka H, Dhonukshe P, Brewer PB, Friml J (2006) Spatiotemporal asymmetric auxin distribution: a means to coordinate plant development. *Cellular and Molecular Life Sciences*, 63:2738–2754. https://doi.org/10.1007/s00018-006-6116-5

Teichmann T, Bolu-Arianto WH, Olbrich A, Langenfeld-Heyser R, Göbel C, Grzeganek P, Feussner I, Hänsch R, Polle A (2008) GH3::GUS reflects cell-specific developmental patterns and stress-induced changes in wood anatomy in the poplar stem. *Tree Physiology*, 28(9):1305-15. https://doi.org/10.1093/treephys/28.9.1305

Theorell H, Ehrenberg A (1952) Magnetic properties of some peroxide compounds of myoglobin, peroxidase and catalase. *Archives of Biochemistry and Biophysics*, 41(2), 442-461. https://doi.org/10.1016/0003-9861(52)90473-6

Thimann, KV (1969) The auxins. In: Wilkins, M. B., ed. *The Physiology of Plant Growth and Development*. McGraw-Hill Publishing Company Limited, London. pp. 1–45.

Tsutsumi Y, Nishida T, Sakai K (1994) Lignin biosynthesis in woody angiosperm tissues III. Isolation of substrate-specific peroxidases related to the dehydrogenative polymerization of sinapyl and coniferyl alcohols from Populus callus cultures. *Mokuzai Gakkaishi* 40: 1348-1354

Tsutsumi Y, Matsui K, Sakai K (1998) Substrate-Specific Peroxidases in Woody Angiosperms and Gymnosperms Participate in Regulating the Dehydrogenative Polymerization of Syringyl and Guaiacyl Type Lignins. *Holzforschung*, 52(3), 275–281. https://doi.org/10.1515/hfsg.1998.52.3.275

Ulmasov T, Murfett J, Hagen G, Guilfoyle TJ (1997) Aux/IAA proteins repress expression of reporter genes containing natural and highly active synthetic auxin response elements. *The Plant Cell*, 9(11), 1963-1971. https://doi.org/10.1105/tpc.9.11.1963

Vanneste S, Friml J (2009) Auxin: a trigger for change in plant development. *Cell*, 136:1005–1016. https://doi.org/10.1016/j.cell.2009.03.001

Vatulescu AD, Fortunato AS, Sá MC, Amâncio S, Ricardo CP, Jackson PA (2004) Cloning and characterisation of a basic IAA oxidase associated with root induction in *Vitis vinifera*. *Plant Physiology and Biochemistry*, 42:609–615. https://doi.org/10.1016/j.plaphy.2004.06.009

Vitha S, Beneš K, Michalová M, Ondřej M (1993) Quantitative β-glucuronidase assay in transgenic plants. *Biologia Plantarum,* 35, 151–155. https://doi.org/10.1007/BF02921141

Waldrum JD, Davies E (1981) Subcellular Localization of IAA Oxidase in Peas. *Plant Physiology,* 68(6):1303-7. https://doi.org/10.1104/pp.68.6.1303

Weinstein LH; Porter CA; Laurencot HJ (1962) Role of the Shikimic Acid Pathway in the Formation of Tryptophan in Higher Plants : Evidence for an Alternative Pathway in the Bean. *Nature*, 194 (4824): 205–206. https://doi.org/10.1038/194205a0

Welinder KG (1992) Superfamily of plant, fungal and bacterial peroxidases. *Current Opinion in Structural Biology*, 2(3), 388-393. https://doi.org/10.1016/0959-440X(92)90230-5

Went FW, Thimann KV (1937) Phytohormones. *Phytohormones*. MacMillan Company, New York.

Yamauchi K, Yasuda S, Hamada K, Tsutsumi Y, Fukushima K (2003) Multiform biosynthetic pathway of syringyl lignin in angiosperms. *Planta*, 216, 496–501. https://doi.org/10.1007/s00425-002-0865-7

Yoshikay-Benitez DA, Yokoyama Y, Ohira, K, Fujita K, Tomie A, Kijidani Y, Shigeto J, Tsutsumi Y (2022) *Populus alba* cationic cell-wall-bound peroxidase (CWPO-C) regulates the plant growth and affects auxin concentration in *Arabidopsis thaliana*. *Physiology and Molecular Biology of Plants,* 28, 1671–1680. https://doi.org/10.1007/s12298-022-01241-0

Zhang J, Lin JE, Harris C, Campos Mastrotti Pereira F, Wu F, Blakeslee JJ, & Peer WA (2016). DAO1 catalyzes temporal and tissue-specific oxidative inactivation of auxin in *Arabidopsis thaliana*. *Proceedings of the National Academy of Sciences*, 113(39), 11010-11015. https://doi.org/10.1073/pnas.1604769113

Zhang L, Wang T, Jiao S, Hao C, Mao Z (2007) Effect of Steam-Explosion on Biodegradation of Lignin in Wheat Straw. *ASAE Annual Meeting*, 077076. https://doi.org/10.13031/2013.22959

Zipor G, Oren-Shamir M (2013) Do vacuolar peroxidases act as plant caretakers? *Plant Science*, 199–200:41–47. https://doi.org/10.1016/j.plantsci.2012.09.018